UNIVERSITY OF SOUTHAMPTON

ANALYSING GAIT FEATURES VIA DATA-DRIVEN APPROACHES

by

Wan Noorshahida Mohd-Isa

A thesis submitted in partial fulfilment of the
requirements for the degree of
Masters of Philosophy

in the
Faculty of Engineering, Science, and Mathematics
School of Electronics and Computer Science

July 9, 2004

UNIVERSITY OF SOUTHAMPTON

ABSTRACT

FACULTY OF ENGINEERING, SCIENCE, AND MATHEMATICS
SCHOOL OF ELECTRONICS AND COMPUTER SCIENCE

Masters of Philosophy

by Wan Noorshahida Mohd-Isa

Work in this thesis is about analysing two types of kinematics data representation: spatial representation and temporal representation. Spatial representation data is proposed to be silhouette moments data and temporal representation data is proposed to be angular displacements data. These data are analysed through a data-driven approach, which employs Principal Component Analysis (PCA) and Canonical Analysis (CA). PCA is a feature representation technique, which aims at reducing input data dimensionality without sacrificing the discriminative capability of the input data information; while CA is a feature discrimination technique, which aims at discriminating the input data for the best possible projection into the feature space. Before the input data are applied to the PCA and CA algorithm, they are pre-processed in a cycle extraction procedure, which involves interpolation and resampling, to ensure the analysis is invariant to different start and end points of a gait cycle. Previous approaches in gait recognition research have depended upon heel-strike frames to determine a gait cycle. Thus, this cycle extraction procedure can relieve this dependability. Results on using the proposed features (angular displacements and silhouette moments) have shown potential and performance is comparable to other literatures. Angular displacements features achieved 98% classification and silhouette moments features achieved 91% classification on a sample database of 10 subjects with 14 sequences each. Findings have shown that angular displacements data is a much better data representation than silhouette's moments.

TABLE OF CONTENTS

LIST OF FIGURES

LIST OF TABLES

ACKNOWLEDGMENTS

I am indebted to my supervisor, Dr. Steve Gunn, for his undivided attention, understanding, and most of all his patience for dealing with my circumstances throughout my study. I also wish to express my appreciation to Professor Mark Nixon, my second supervisor, for his guidance, and especially his help on getting me the maintenance grant, which had helped me in sending my first daughter to the nursery during my final two years of study. My thanks go to Dr. Adam Prügel-Bennett for examining my work and giving his comments in the vivas. Also thanks to Dr. Christine Shadle for her advice when dealing with matter regarding maternity leave of my new daughter.

To these people, who used to work in ISIS; Dr. Chew-Yean Yam, for her comments on my work that had led me to look at my work differently; Dr. Mike Grant, for his help on getting data clusters in Barman; and Dr. Jeff Foster, for his explanation on PCA and CA.

Most of all, I would like to express my gratefulness to God, for allowing me to think, see, and take things positively during the course of my study. This thesis is dedicated especially to my first daughter, Atiqah, for I have not been the perfect mother for her at times. Last but not least, thanks to my husband, Junaidi, for his constant support, and new daughter, Nafisah, for her smiles have always made my day.

NOMENCLATURES

θ	- hip angle
ϕ	- knee angle
ρ	- ankle angle
S_H	- hip point label
S_K	- knee point label
S_A	- ankle point label
S_{OE}	- toe point label
m_{pq}	- binary image Cartesian moment function
μ_{pq}	- centralised binary image Cartesian moment function
p,q	- moment order number
M	- image dimension (horizontal pixels)
N	- image dimension (vertical pixels)
L	- number of image frame of a sequence
S	- number of sequence of a subject
S_T	- total number of sequences of a dataset
C	- number of subject of a dataset
$\mathbf{M}_{pq}$	- moment order $(p+q)$ matrix
$K(t_i,t)$	- kernel function
α_i	- support vectors
t_i	- time of each angular displacements/silhouette moments
r	- resampled length of a sequence
$\mathbf{X}$	- input dataset into PCA
$\mathbf{x}_{ij}$	- input vector for class i sequence j into PCA
$\mathbf{Y}$	- projected dataset by EST
$\mathbf{y}_{ij}$	- projected vector for class i sequence j by EST
$\mathbf{z}_{ij}$	- projected vector for class i sequence j by EST + CST
$\mathbf{S}_w$	- CA within-class matrix
$\mathbf{S}_b$	- CA between-class matrix
λ_i	- eigenvalue
$\mathbf{e}_i$	- EST vector
$\mathbf{w}_i$	- CST vector
k_λ,	- number of features to use
K_λ	- total number of features available
p_λ, P_λ	- truncation percentage of eigenvalues
k	- nearest neighbour

Chapter 1

INTRODUCTION

"Automatic identification represents a set of technologies that (to the uninitiated) seems to work like magic." [Swartz 1999]

1.1 Background

Since the event of September 11, discussion on biometrics has becoming increasingly popular among government agencies, commercial companies, not forgetting the researchers! Biometrics is seen to (perhaps) provide solutions for securing data and facilities that are vulnerable to terrorists' attack, which is believed to be the culprit behind this historical event. Its technology aims to identify people by their physical traits, the most commonly applied being fingerprints, faces, irises, voices, DNAs, and next is gait.

The Oxford dictionary defines gait as "manner of walking, bearing, or carriage as one walks". As a biometric, gait may be defined as a means of identifying individuals by the way they walk [Nixon et al. 1999]. It is known to be one of the most universal and complex of all human activities, and each person appears to have his or her own characteristic gait pattern [Murray et al. 1964] [Inman et al. 1981] [Eng and Winter 1995]. Medical studies including biomechanics scientists and psychologists have involved many years in this discipline [Murray et al. 1964] [Inman et al. 1981] [Eng and Winter 1995] [Stevenage et al. 1999].

Fingerprint recognition requires scanners, which a person needs to touch, as tool for its identification, which for some people may seem intrusive, then gait is a more attractive identification system since it operates on video cameras, thus it is non-invasive and recognisable over a distance. Therefore gait technology is suitable for security and monitoring systems since a "bunch of

terrorists" in action may wear masks and/or gloves to disguise face recognition and/or fingerprint recognition system. However video cameras in a surveillance system can almost always have their views obstructed by decorative plants, and/or have their depictions blurred and indistinct. Gait can also handle these occlusions and noises in the video cameras.

Additionally gait itself is self-occluded at some points while in motion. Fortunately, it is difficult to conceal as it is inherent in a person's motion and its symmetrical and periodic structure allows for reconstruction of 'missing' or 'noisy' views. Hence, it has several advantages over other biometrics when applied in automatic identification systems.

1.2 Automatic Gait Recognition

A study on automatic gait recognition is an applied pattern recognition problem and can be defined to be,

> a study of how machines can observe gaits, learn to distinguish its patterns of interest, and make sound and reasonable decisions about the classes of these patterns.

A generic automatic gait recognition system can be viewed as in Figure 1.1 and involves the common sensor, feature extraction, and classifier elements.

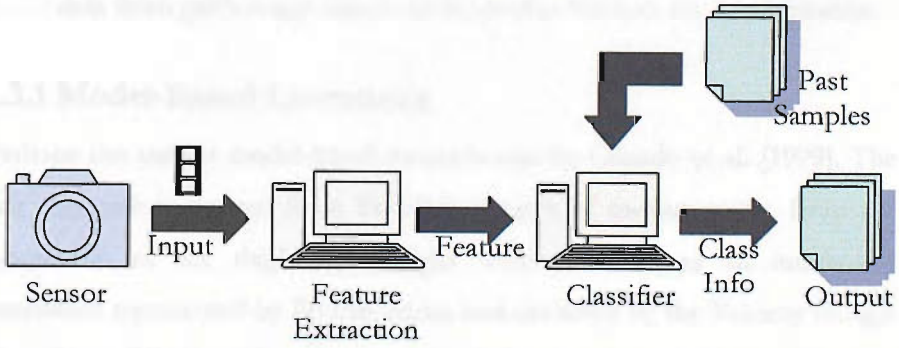

Figure 1.1. A generic automatic recognition system.

The sensor is normally a video camera(s), which could come from a common surveillance system in a typical approach. The inputs are video clips cum image frames of a walking person and these undergo a process of feature extraction (or selection) for obtaining useful features, which are compressed inputs, in a computer. At the next stage, the features are applied to a classifier where past samples assist in discriminating them and assign them a class label, which then becomes the output of the recognition system. All processes are done automatically by computers. Also it should be noted that the success of the next stage of each process depends highly upon the performance of the previous process (es).

1.3 Automatic Gait Recognition Literatures

Numerous literatures on automatic gait recognition date as far back as 1994, and can be divided into two main approaches: the model-based approach and the data-driven approach.

> **The model-based approach** emphasises the representation of the biomechanics of gait by a mathematical physical model. This approach models motion of the limbs while a person is walking (or running) and formulates a mathematical description of these features.

> **The data-driven approach** emphasises the derivation of statistical information from a set of extracted gait data. This approach extracts data from gait's image frames to be used as features for discrimination.

1.3.1 Model-Based Literatures

Perhaps the earliest model-based research was by Cunado et al. [1999]. The gait signature is derived from Fourier's spectra of measurements from the orientation of the thigh. The thighs were modelled as an interlinked pendulum represented by Fourier Series and extracted by the Velocity Hough Transform (VHT). The phase-weighted Fourier magnitude spectra came from the changes on thigh angular displacements by edge detection. The

recognition rate is 90% on a small database of 10 subjects 4 sequences each, using *k*-nearest neighbour classifier.

Another development models both the upper and lower leg of walking and running subjects as two inter-connected penduli using a bilateral symmetric and dynamically coupled oscillator [Yam et al. 2001] [Yam 2002]. The gait signature is the phase-weighted magnitude of the frequency components of limbs' angular movement. The recognition rate reached 96% for walking and 92% for running for 5 subjects 5 sequences each, respectively.

A more recent work is on a marker-less gait recognition system by combining a statistical approach and motion tracking with topological analysis guided by anatomical knowledge [Yoo et al. 2002] [Yoo and Nixon 2003]. The marker-less system describes periodic gait motion by its symmetry and fits a 2D stick figure to the gait data. This system consists of three key stages: detection and extraction of the moving body and its contour; extraction by the joint angles and body points; and kinematics analysis and feature extraction for classifying the gait pattern. The signatures are 20 different features based on kinematics analysis of one gait cycle and the performance varied from 82% for 100 subjects 3 sequences each to 93% for 100 subjects 2 sequences each. However, performance on a small database of 10 subjects produced 100%.

1.3.2 Data-Driven Literatures

Much research is data-driven. Among early research in automatic gait recognition is the work by Niyogi and Adelson [1994], in which the gait signature is derived from the walking patterns in a spatio-temporal volume. These patterns were used to determine the motion's bounding contours. The gait vectors were derived by using linear interpolation after normalising a fitted five-stick model for velocity. The recognition rate varied from 60% to just over 80% on a database of 5 subjects 26 sequences each.

Research from Murase and Sakai [1996] used the parametric eigenspace approach, an approach well established in automatic face recognition. They derived body silhouettes by subtracting adjacent images and projected them into the eigenspace. Decomposition of the eigenvalues reveals the silhouettes' frequency content, which corresponds to the order of the eigenvectors. The recognition rate varied from 88% to 100% depending on the number of eigenvectors used. The database had 7 subjects 10 sequences each.

Little and Boyd [1998] measured the difference in phase of optical flow images to derive the gait signature. The optical flow produced a set of moving points together with their flow values. A periodic structure of the sequence was derived from the measurement of the geometry of the set of points. Analysis on the periodic structure produced several irregularities in the phase differences, which includes the differences in phase between the centroid's vertical component and the phase of the weighted points. The recognition rate is 95% on a limited database of 6 subjects 7 sequences each.

Further, Huang [1999] combined the Principal Component Analysis (PCA) and Canonical Analysis (CA) for gait recognition. PCA was selected as the first stage of feature extraction for the purpose of dimensionality reduction. The second stage applied the projected features to CA for discriminating different classes further in the feature space. The recognition rate varied from 76% to 100% depending on the features used. The features were human silhouettes, which are the spatial template and optical flow between two consecutive silhouettes, which are the temporal templates. The so-called extended features of combining both spatial and temporal template produced the 100% recognition rate. The technique was applied to two databases: UCSD with 6 subjects 7 sequences each and SOTON with 6 subjects 4 sequences each.

There is additional data-driven research on using moments (or its variations) of silhouettes as gait signatures such as the work of Shutler et al. [2000a]

[2000b], which employed velocity moments to describe gait and its motion throughout the image sequences. His work achieved over 90% recognition rate for the first four moment features on a small database. Prismall et al. [2002] [2003] used the orthogonal Legendre and Zernike moments to describe moving shapes and predict missing or intermediate frames within a sequence for further reconstruction. His work had shown that high order moments could accurately reconstruct binary images. Work by Lee and Grimson [2002a] [2002b] took several simple moment-based features as signatures to recognise subjects by gait appearance. The moments were extracted at different regions of silhouettes. The silhouettes were divided into seven regions and ellipses were fitted to each region. The moment centroid, aspect ratio of the ellipse's major and minor axis and orientation of the ellipse's axis were among the sets of 41 and 57 features extracted. The performance evaluation was based on cumulative match score described by Philips et al. [1997] and was 100% on the set of 41 features for the first match and 97% on the set of 57 features for the first match and 100% for the third match. The number of subjects is 24 with different number of sequences for different subjects but on average has eight number of sequence.

1.3.3 Comments on Literature Review

A model-based approach is object-specific, such as the work of Cunado [1999] and Yam [2001] [2002] that specifically model the thigh and the lower leg as an interlinked pendulum. Their works have managed to formulate gait mathematically through looking at the structure underlying the gait pattern but lacks the statistical and intimate nature of gait. Thus, with other gait patterns, for example a quadruped like an animal, new models need to be derived. A data-driven approach is more holistic and flexible, which aims at deriving mathematics models based on the statistical nature that exists in the data. Thus, this work employs the data-driven approach into analysing gait.

There is research in automatic gait recognition on both model-based and data-driven approaches that are worth mentioning. The other research

showed promising results aimed at analysing gait data for its potential as a biometric. Below is a summary on the literature review, which motivates and relates to the work of this thesis:

- The works of Cunado [1999] and Yam [2001] [2002] have motivated the use of angular displacement data of the thigh and lower leg. Both are model-based approach, which obviously modelled the biomechanics of gait as an interlinked pendulum but only limited to the orientation of the thigh and lower leg. However, the biomechanics of gait involves complex interaction of muscles, joints, and force acting on the body, which includes pelvic rotation, pelvic tilt, knee flexion, foot and ankle motion, knee motion, and lateral pelvic displacements. Thus, in this work, extended features are proposed, which is the foot flexion and the combination of angular displacements.

- Work of Niyogi and Adelson [1994] derived the gait patterns in the spatio-temporal volume by normalising and using linear interpolation of the gait vectors. Normalisation and interpolation are basic mathematical techniques for standardising sets of scattered data. Hence, the cycle extraction is formulated so as to apply them to the gait feature vectors for invariant analysis.

- Murase and Sakai [1996] and Huang [1999] have used the eigenvectors projection method, which is a successful and popular method in automatic face recognition [Swets and Weng 1996] [Belhumeur et al. 1997] [Zhao et al. 1998] [Zhao et al. 2000] [Martinez and Kak 2001] [Beveridge et al. 2001] [Chen and Man 2003]. Likewise, their approaches in gait research have been successful. Thus, the work of this thesis employs this standard eigenvector projection method for its descriptor analysis but applied to different feature vectors.

- The result of phase difference in the work by Little and Boyd [1998] has led to the investigation of the difference of the feature vectors phase direction in the descriptor analysis. This motivated the need to uniformly extract gait cycles with similar phase throughout the dataset.

- The analysis on silhouette moments in this work is motivated by the work of Shutler [2000a] [2000b], Prismall et al. [2002] [2003], and Lee and Grimson [2002a] [2002b]. They have successfully employed different silhouette moments; namely velocity moments, Legendre and Zernike moments, and Cartesian moments. In addition silhouette data is easily gathered than manually labelled angular displacement data, which allows for future analysis with increase sample size.

- Most research has successfully used a small number of subjects with a small number of sequences except in the work by Yoo et al. [2002] [2003] and Lee and Grimson [2002a] [2002b], which has at least 200 and 192 numbers of total sequences, respectively. Thus, this research proposed to apply to a dataset with 140 total sequences containing 10 subjects with 14 sequences each.

1.4 Data-Driven Approach System

Data-driven analysis is concerned with deriving statistical information from a set of extracted data. Statistical information may include measuring the mean, variance, and analysing correlation from scatter of a set of readings. A data-driven-approach system aims at producing an informed decision on class labels of new or 'unseen' input data by processing it and testing it against systematically gathered and analysed past samples. The processes involve minimising the probability of misclassification, which fundamentally would be to minimise the Bayes error.

A data-driven-approach system employs the similar system as in Figure 1.1. Figure 1.2 is a thumbnail of the data-driven-approach system, which describes

the work in this thesis. Based on that figure, the problem of classification in a data-driven-approach can be defined as,

> the mapping of a high-dimensional gait input data x to its one-dimensional subject label c.

The system is divided into two parts: training and testing. The training part involves processes that observe gait input data and then analyse them for distinguishing their patterns of interest. On the other hand, the testing part uses the patterns that have been analysed by the training part to further classify new data according to their identities. The processes involved in both training and testing is described in the following sections.

1.4.1 Data Acquisition and Collection

As a first process, the system captures gait videos, which becomes the input data. Most of the time, a pre-processing is done to the input data, which may include extraction of the videos into image frames, adjustments for average intensity levels on the image frames, adjustments for standard image frames size, and segmentation to isolate the subjects from its background in the case of producing silhouettes. After this process, the input data is commonly known as raw data.

There are two types of collected data: supervised and unsupervised. Supervised data has known target values, i.e. labelled output values, which are provided by experts in that particular area or are generated by measurements. Unsupervised data has no target values. For gait recognition, its data can be both types depending on how the data is collected. In this thesis the data has target values that is the class label is associated with the subject and so the problem is one of supervised classification.

Gait data in this thesis consist of 10 walking subjects with 14 sequences for each subject; nine male subjects and one female subject. The 14 sequences include seven sequences of subjects walking from left to right and seven

sequences of subjects walking from right to left. The gait data set is selected randomly from a gait database developed for DARPA Human ID Projects [Shutler et al. 2002]. Part of the database in the DARPA Project is developed by the ISIS (Image, Speech, and Intelligent Systems) Research Group, University of Southampton, UK.

The data set selected in this work is filmed indoors with controlled lighting, fixed green background, and a defined walking track. The subjects walk normal to the view of a stationary DV (digital video) camera with imaging frequency of 25Hz and a resolution of 720 x 576 colour pixels. The subjects are filmed side-viewed as video clips, which are then digitised into individual image files. The video captures about two complete gait cycles.

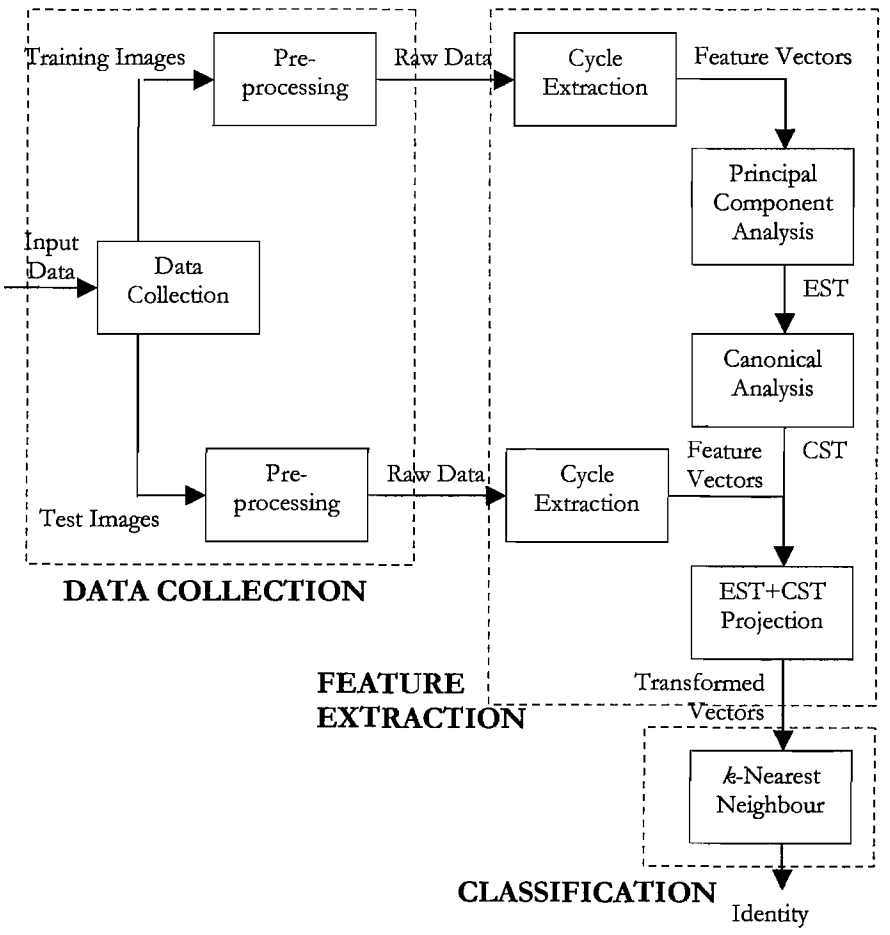

Figure 1.2: Thumbnail of system describing work in this thesis.

Silhouette dataset in this thesis is generated from this original image. It is used by many in gait recognition researches [Murase and Sakai 1996] [Huang 1999] [Shutler et al. 2000a] [Shutler et al. 2000b] [Abdelkader et al. 2002a] [Abdelkader et al. 2002b] [Lee and Grimson 2002a] [Lee and Grimson 2002b] [Mowbray and Nixon 2003] [Prismall et al. 2002] [Prismall et al. 2003] [Bhanu and Han 2003]. Each silhouette is produced by first isolating the subject from its background and then performing background extraction via chroma-keying on each image. Finally each image is threshold to produce a silhouette. Each silhouette retains its size of 720 x 576 pixels.

In this work, the collected raw data are the angular displacements and silhouette moments data. They are kinematics characteristics from gait motion patterns. Kinematics characteristics concern the geometry of the motion without reference to force, which produces the motion and mass of the subject while in motion. The kinematics traits can be further categorised into spatial representation and temporal representation based on the content of gaits image frames. Spatial representation includes position, silhouette region, and boundary of a gait image. While temporal representation includes velocity, accelerations, and angular displacements.

The angular displacements data contains angles of displacements for the thigh, the lower leg, and the foot at each individual image frames. Based on research by Johansson [1973], human motions of points can be distinguished from other non-biological motions. Moreover angular displacements of the thigh and lower leg have been used in many studies [Murray et al. 1964] [Grieve and Gear 1966] [Murray 1967] [Frigo et al. 1986] [Hills and Parker 1993] [Eng and Winter 1995] [Cunado et al. 1999] [Lakany 2000] [Yam 2002]. Hence, the angles of displacements are calculated from manually labelled points at the hip, knee, ankle, and toe for the corresponding image frames.

The silhouette moments data contains Cartesian centralised moments of silhouette at each individual image frames. Image moment representations

have been found to be useful in many pattern recognition applications. They are popular with a statistical pattern recognition approach since a major assumption is that there is an unoccluded view of target shape [Nixon and Aguado 2002]. Moments, which describe an object layout by its pixels, are a global descriptor. They have invariance properties and a compact description, which can avoid the effects of noise in description. The Cartesian centralised moments are translation invariant, thus by employing image moments, the translation of silhouette image frames in time can be represented accurately up-to a certain well-defined order.

The silhouette moments data and the angular displacements data are further processed for extraction and selection of useful features as described in the next section. Their mathematical formulation is described in **Chapter 2.**

1.4.2 Feature Extraction and Feature Selection

Gait input data is high dimensional. A digital video of one gait cycle normally extracts into hundreds or thousands of image frames of standard dimensions. Only specific features of gait are extracted or selected depending upon the need of the systems whether to employ feature extraction or feature selection techniques. Both techniques lead to dimensionality reduction of data.

Feature extraction relates to techniques that use a class separability optimality criterion to generate a mapping from the input data space to the feature space [Young and Fu 1986]. Feature extraction creates new features by transformations or combinations of the existing input data. Feature selection differs from feature extraction in that it chooses features but the ones more informative from the set of the new features. It identifies the most important and relevant input variables that are responsible for major variations of the output. However different in names they are, the motivation behind these techniques is to reduce or compress the amount of raw data utilised for further processing. It is a known fact that the amount of data relates to the complexity of the system, which relates to performance and cost of the

system. The term 'curse of dimensionality' is common in pattern recognition where an increase in the dimensionality of the features means an exponential increase in generalisation process [Bellman 1961].

It is important to note that depending upon the criteria measured by the mapping function, feature extraction techniques can be further categorised into feature extraction for representation and feature extraction for classification. For representation purpose, the goal is to map the input data accurately in the lower-dimensional feature space. Whilst for classification purpose, the goal is to enhance the class-discriminatory information in the lower-dimensional feature space. Examples of techniques are Principal Component Analysis (PCA) and Canonical Analysis (CA), which are techniques used in this work. The former is a feature extraction technique for representation and the latter is a feature extraction technique for classification.

The principal component analysis (PCA) is a transformation based on statistical properties of vector representations [Gonzales and Woods 1992]. Also known as the Karhunen-Loeve transformation, PCA transforms continuous data into a set of uncorrelated coefficients by using the transformation matrix of eigenvectors. The covariance matrix of the data set generates these eigenvectors and its corresponding eigenvalues. These eigenvectors can be ordered according to their eigenvalues, which measure the variance of the transformed vectors along these eigenvectors. Thus, the first transformed vector, or the principal component, shows the direction of maximum variance, which yields projection directions that maximise the total scatter across all data. The principal components of very low variance can be removed, as they do not contribute much to the projection of the data. Hence, PCA has the capability for performing data compression.

Canonical analysis (CA) is an established technique, which aims to determine whether two or more sets of objects differ from each other [Ehrenberg 1989]. The method discriminates data while keeping the intra-variance minimum and

the inter-variance maximum. To do that, CA computes the ratio of the within-class to the between-class scatter and employs a generalised linear discriminant function to maximise this ratio simultaneously. The solution to this analysis is an orthogonal basis, which spans the canonical space. Projection of vectors into this canonical space can produce clusters of disparate vectors with low intra-variance and high inter-variance.

Huang [1999] has derived a method, which combined both PCA and CA. The combination of PCA+CA performs better discrimination of different classes than the CA method alone. Furthermore, employing PCA first can avoid the singularity problem in computation of the within-class scatter with uncompressed data in CA. Therefore, PCA does data compression that reduces the amount of the input data, which is high-dimensional by retaining data which accounts for most variance. When CA is applied to such data, it discriminates better. In his work, the combination of PCA and CA was used for gait recognition on silhouette data and optical flow of silhouette data. Huang used the image itself; the silhouette, which is computed from the subtraction of the background image from the objects in the image and optical flow, which is computed from the displacement of each pixel between each silhouettes. In this work, the combination of PCA and CA is used for analysing angular displacements and silhouette moments data.

Before these raw data, namely the angular displacements and silhouette moments data are analysed by the feature extraction techniques, they are pre-processed to detect and remove any potential outliers, which can affect the mapping of the feature vectors in the feature space. Outliers are unusual data values that are inconsistent with most observations. They can be due to gross measurement errors, coding/encoding errors, and abnormal cases. Also, pre-processing involves making the feature extraction analysis invariant to different temporal and/or spatial information contained in the raw data. With gait data, one possible method of pre-processing before feature extraction is to employ the cycle extraction procedure.

1.4.3 Classifiers

Classification of the extracted or selected features is the last stage in the system. At this stage the gait features are assigned class or subject label by the chosen classifiers, which use certain criteria of separability measures. Gait features with its associated class/subject label are known as patterns and these patterns are used to design the classifier (or to set its internal parameters) [Webb 1999]. In the future new gait data may be generalised to its class association using the designed system.

However, the design of classifiers is not the work of this thesis. Therefore, the commonly used *k*-nearest neighbour classifier with Euclidean distance is employed as its classifier due to its simplicity.

1.5 Significance of Problem

This thesis focuses on analysing gait features using data-driven approach. It aims at answering the question on how descriptive is gait by studying its features. Gait motion pattern can be described by its kinematics characteristics, which concern the geometry of the motion. The kinematics traits can be further categorised into spatial representation and temporal representation. Spatial representation includes silhouette region and boundary of a gait image. While temporal representation includes velocity and angular displacements. Gait features can be extracted or selected from any of these representations thus an analysis on how these features successfully discriminate gait is discussed in this thesis. A data-driven approach is employed for investigating these gait features, namely using Principal Component Analysis (PCA) and Canonical Analysis (CA). PCA and CA are both feature extraction techniques, where the former is a technique for representation of the input data that can be used for dimensionality reduction, while the latter is a technique for discriminating the input data for better classification.

The input data in this thesis are the angular displacements and silhouette moments. We choose the angular displacements of the thigh and knee for they are consistent with many studies [Murray et al. 1964] [Grieve and Gear 1966] [Murray 1967] [Frigo et al. 1986] [Hills and Parker 1993] [Eng and Winter 1995] [Cunado et al. 1999] [Lakany 2000] [Yam 2002], which show that they are quantifiable. The work extends into investigating the flexion of the foot throughout a gait cycle and the combination of the three angular displacements. We choose silhouettes for they are used in many gait recognition literatures [Murase and Sakai 1996] [Huang 1999] [Shutler et al. 2000a] [Shutler et al. 2000b] [Lee and Grimson 2002a] [Lee and Grimson 2002a] [Prismall et al. 2002] [Prismall et al. 2003] [Bhanu and Han 2003]. It also has the advantage of having large sample size because it is easily gathered than manually labelled limb angular displacements. However, silhouette moments are used due to constraints on processing large two-dimensional data size. Thus, the analysis investigates and compares the performance of differing input data.

As gait is periodic, cycle extraction analysis is proposed for extracting gait cycles from the discrete signal representing the input of gait kinematics data. The cycle extraction procedure involves interpolation and resampling of the discrete signal. Cubic spline interpolation in SVR (Support Vector Machines for Regression) is proposed since it handles the start and end points for gait cycle extraction much better than normal cubic spline interpolation. The gait cycle is extracted to be between two consecutive zero crossings, which complete a gait cycle and resampling is performed for uniformity of sample size due to differences in walking speed. This technique relieves the analysis from dependence upon heel-strike, which was employed in previous research. Also, in this part of the analysis, the input data is extracted to have similar phase direction throughout the dataset since a difference in phase can affect the distribution of the input data in the feature space, which in turn can affect the recognition process.

Contributions of this thesis are laid out as follows:

- The proposal of using angular displacements data for analysis on the PCA and CA analysis by Huang [1999]. Huang's analysis used silhouettes and optical-flow of silhouettes data. The angular displacements involve are the hip, knee, and ankle.

- The proposal of using silhouette moments for comparison analysis with the angular displacements data.

- The proposal of cycle extraction method using combination of SVR and resampling at zero crossings. This method deals with defining different start and end points to determine a gait cycle other than formerly depending on heel-strike.

1.6 Thesis Preview

The outline of the thesis is as follows:

Chapter 2 describes theoretical material on gait's input data: angular displacement data and silhouette moment data; what they are and how they are collected and pre-processed for feature extraction. This chapter also presents the theoretical methods for analysing their features, which are the PCA and CA algorithm.

Chapter 3 formulates cycle extraction method, which involves description of cubic spline interpolation in SVR and resampling at zero crossings. The results are presented for both types of input data from **Chapter 2.**

Chapter 4 presents the overall results of this thesis, which includes comparison results for each input type of gait's data. Also discusses on findings and comparing to other gait literatures.

Finally **Chapter 5** concludes the thesis and outlined the future work.

Chapter 2

MATHEMATICAL FORMULATION OF GAIT'S DATA AND ITS DESCRIPTOR ANALYSIS

This chapter presents theoretical and mathematical formulation for both angular displacements and silhouette moments data. Also, it describes descriptor analysis, namely the PCA and CA, which are employed for feature extraction process in the data-driven approach system.

2.1 Gait's Data

Murray [1967] considered gait to be "a total walking cycle – the action of walking can be thought of as a periodic signal". The period of a gait cycle exists between successive heel-strikes. Also, the cycle has two phases: the stance phase and the swing phase. The stance phase is the duration when the foot is on the ground, whilst the swing phase begins with the toe-off of that foot. This is illustrated in Figure 2.1.

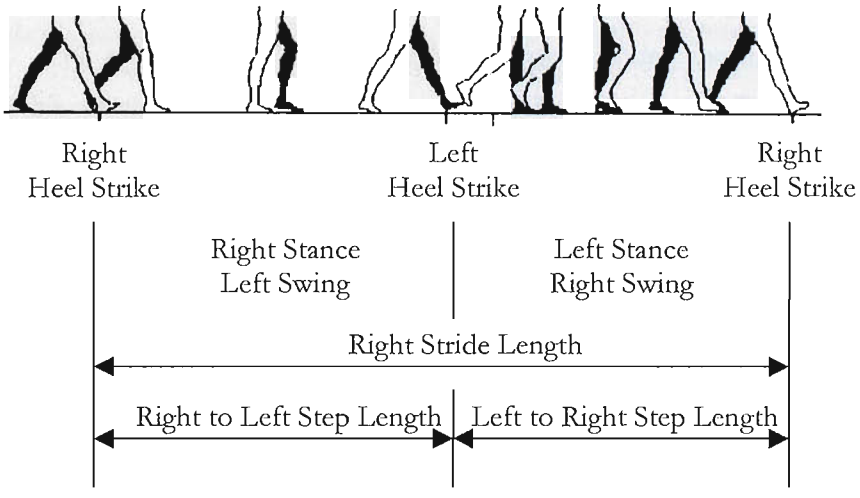

Figure 2.1: Duration of total right walking gait cycle.

In Figure 2.1 the gait cycle begins with the heel strike of the right leg and the person enters the stance phase of walking. In this phase, the body weight shifts onto the foot when the foot falls flat. Then, the left leg swings to the front and body reflexes make the right foot flat because the body weight has shifted to the right leg. The stance phase ends when the right foot, which moved first lifts again; the swing phase starts when the left toes lift from the ground. That completes one step. Then, the body weight shifts and the leg swings to the front again. The stride ends when the heel of the right foot, which moved first strikes the floor again. That completes the other step and the gait cycle.

A gait cycle can be described by its kinematics characteristics, which concern the geometry of the motion without reference to force. The kinematics characteristics can be further represented spatially or temporally. Angular displacements data is proposed as temporal representation of gait periodic signal and silhouette moments data is proposed as spatial representation of gait periodic signal. Their formulation is described in the next section.

2.1.1 Angular Displacements Data

Geometrically, the maximum opening of the legs are when the leg is at heel strike. The minimum opening of the legs happens during the leg swing. From this geometry, Figure 2.2 is constructed. The data is manually labelled at each individual image frames corresponding to the leg at front (refer Figure 2.2(b)) at four points; the hip S_H, the knee S_K, the ankle S_A, and the toe S_{OE} as in Figure 2.2(b). The hip angle θ, is the angle of inclination between the thigh and the vertical while in motion. The knee angle ϕ, is the angle at the knee between the lower leg and the vertical. The ankle angle ρ, is the angle of the foot flexion with respect to horizontal. Then, the co-ordinates of these points are gathered and used to calculate the angles of inclination θ, ϕ, and ρ. These angles are illustrated in Figure 2.2(a).

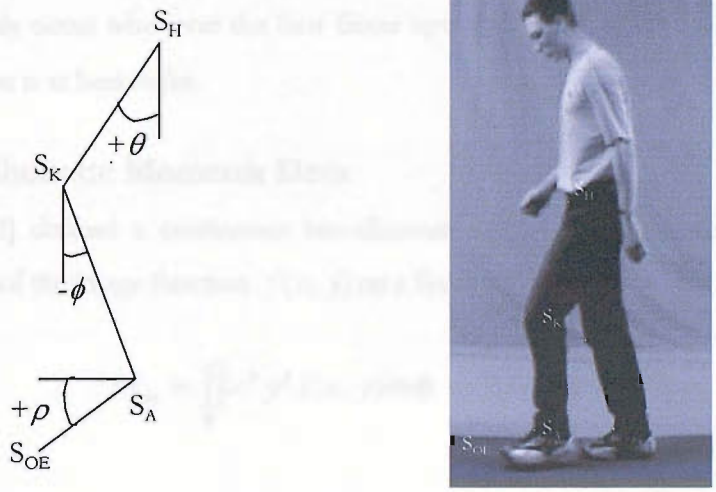

(a) Location (b) Example

Figure 2.2: Labelled points on digitised image.

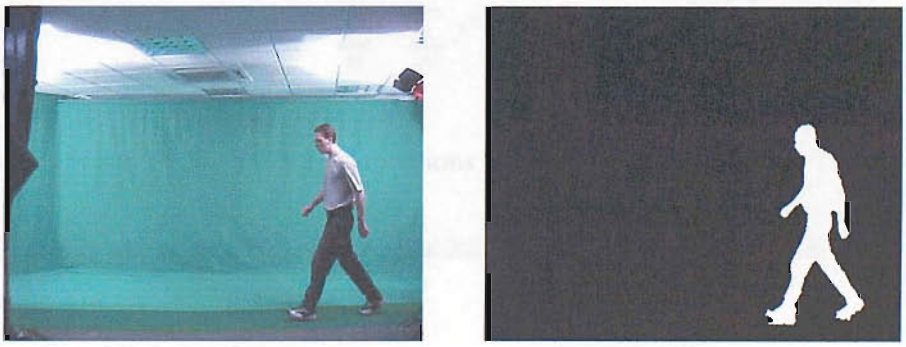

(a) Original Image (b) Silhouette

Figure 2.3: Original image and its corresponding silhouette.

The positive values for θ and ϕ are defined to be whenever the displacement angles are moving forward together with the forward movement of the subject. The positive values for ρ are defined to be at the region whereby the foot of the subject is at its natural position. Therefore negative values for ρ can only occur whenever the foot flexes upwards, which is the time when the person is at heel strike.

2.1.2 Silhouette Moments Data

Hu [1962] defined a continuous two-dimensional $(p+q)$th order Cartesian moment of the image function $f(x, y)$ on a finite region $\Re$ as,

$$M_{pq} = \iint_{\Re} x^p y^q f(x, y) dx dy \tag{2.1}$$

where, $p, q = 0, 1, 2, \ldots$

In a binary image form, $f(x, y) = 1$ represents a shape of the moment in the region $\Re$. Thus, the double integral in Equation 3.1 is replaced by a summation to produce the separable computation,

$$m_{pq} = \sum_{M} x^p \sum_{N} y^q \tag{2.2}$$

where M and N are the image dimensions of the object.

By setting the order $(p+q)$ of Equation 2.2, these moments are useful in shape analysis of our silhouette data.

The order of moments can represent various attributes of an object in an image. For an N pixel shape represented by a region $\Re$, the following attributes are defined:

a. Area

The 0^{th} order moment defines the area of an object. A 0^{th} order moment is obtained by setting $p = 0$ and $q = 0$. Thus, Equation 2.1 becomes,

$$A = M_{00} = \iint_{\Re} f(x, y)dxdy \tag{2.3}$$

For a binary image of N pixels, Equation 2.3 is just the total number of pixels, N, for the object in the binary image.

b. Centre of Mass

The 1^{st} order moment defines the centre of mass or means of the object of interest. Equation 2.1 then becomes,

$$\bar{x} = \frac{\iint_{\Re} xf(x, y)dxdy}{\iint_{\Re} f(x, y)dxdy} \tag{2.4}$$

$$\bar{y} = \frac{\iint_{\Re} yf(x, y)dxdy}{\iint_{\Re} f(x, y)dxdy} \tag{2.5}$$

where $\bar{x}$ and $\bar{y}$ in binary form are $\bar{m}$ and $\bar{n}$ respectively,

$$\bar{m} = \frac{1}{M}\sum_{(m,n)}\sum_{\in\Re} m \tag{2.6}$$

$$\bar{n} = \frac{1}{N}\sum_{(m,n)}\sum_{\in\Re} n \tag{2.7}$$

These $\bar{x}$ and $\bar{y}$; or $\bar{m}$ and $\bar{n}$ represent the centre of mass for the vertical and horizontal direction of the object in an image respectively.

From these equations of centre of mass, Equation 2.2 above can be centralised and become the (p,q) order central moments as,

$$\mu_{pq} = \sum_{(m,n)\in\Re}\sum (m-\bar{m})^p (n-\bar{n})^q \tag{2.8}$$

Equation 2.8 is extensively used throughout the work on silhouette analysis.

c. Directional Variance

The 2^{nd} least order moment defines the spread of the shape with respect to either the vertical or the horizontal direction, or variance. General Equation 2.1 becomes,

$$\sigma_x^2 = M_{20} = \int (x-\bar{x})^2 f(x)dx \tag{2.9}$$

$$\sigma_y^2 = M_{02} = \int (y-\bar{y})^2 f(y)dy \tag{2.10}$$

The binary image form will be,

$$\sigma_m^2 = m_{20} = \sum (m-\bar{m})^2 \tag{2.11}$$

$$\sigma_n^2 = n_{20} = \sum (n-\bar{n})^2 \tag{2.12}$$

2.1.3 Justification for Using Moments of Silhouette

Angular displacements data are measured angles from each image frame. The angles are mapped into a column vector with each item (angle) in the vector representing its image frame. Having many image frames just increases the length of the angle vector. That means a sequence of L image frames is an L length vector.

Silhouette data contains binary image representation of gait image database. It has the advantage of having a large sample size because it is more easily gathered than manually labelled angular displacements data. However, the silhouette dataset in this work uses the same number of subjects and sequences as the angular displacements data. Each original image frame of a silhouette data is of size 720 x 576 pixels. Each of these sequences contains between 50 to 77 image frames.

For the purpose of image analysis, normally an image of size M x N is rearranged to map as a row-ordered vector, or often called the lexicographic ordering[1] [Jain 1989]. By scanning the pixels of an image from the first row, and going from first column till the end, an image of size 720 x 576, will become a long column vector of size 16560. That size is not considering the other L-1 number of image frames, S-1 other sequences, and C-1 other classes! Due to this, the direct computation of the silhouette data into the descriptor analysis algorithm will be enormous. Therefore, moment representation is proposed for analysing silhouette data.

---

[1] Let

$$\mathbf{x} \triangleq O\{x(m,n)\}$$

be a one-to-one ordering of the elements of the array $\{x(m,n)\}$ into the vector $\mathbf{x}$.

The row-ordered vector is defined as

$$\mathbf{x}^T = [x(1,1)x(1,2)\ldots x(1,N)x(2,1)\ldots x(2,N)\ldots x(M,1)\ldots x(M,N)]^T$$
$$\triangleq O_r\{x(m,n)\}$$

The column-ordered vector is defined as

$$\mathbf{x}^T = [x(1,1)x(2,1)\ldots x(M,1)x(1,2)\ldots x(M,2)\ldots x(1,M)\ldots x(M,N)]^T$$
$$= \begin{bmatrix} \mathbf{x}_1 \\ \mathbf{x}_2 \\ \vdots \\ \mathbf{x}_N \end{bmatrix} \triangleq O_c\{x(m,n)\}$$

2.2 Descriptor Analysis

Principal component analysis (PCA) and canonical analysis (CA) are techniques successfully employed in face recognition and object recognition [Swets and Weng 1996] [Belhumeur et al 1997] [Zhao et al 1998] [Zhao et al. 2000] [Martinez and Kak 2001] [Beveridge et al 2001] [Chen and Man 2003]. Both techniques are statistical techniques that can be adopted for a data-driven analysis in automatic gait recognition. In this work, PCA is used as a feature extraction technique for representation of the input data to a reduced dimension. CA is an intuitive feature extraction technique in which minimising the within-class scatter and maximising the between-class scatter of the input data can discriminate the dataset better. The combination of PCA and CA is used for analysing angular displacements and silhouette moments data. PCA is applied first for data truncation, and then CA is performed before the classification process as described in **Section 1.4**.

2.2.1 Principal Component Analysis (PCA)

Given resampled vectors estimate of length r (Equation 3.7 – Equation 3.10, which will be discussed in **Section 3.3.1**), for matrices r x S_T containing vectors of length r representing S_T number of total sequences,

$$\mathbf{X}_{\theta} = [\hat{\boldsymbol{\theta}}_1 \hat{\boldsymbol{\theta}}_2 \ldots \hat{\boldsymbol{\theta}}_{S_T}] \tag{2.13}$$

$$\mathbf{X}_{\phi} = [\hat{\boldsymbol{\phi}}_1 \hat{\boldsymbol{\phi}}_2 \ldots \hat{\boldsymbol{\phi}}_{S_T}] \tag{2.14}$$

$$\mathbf{X}_{\rho} = [\hat{\boldsymbol{\rho}}_1 \hat{\boldsymbol{\rho}}_2 \ldots \hat{\boldsymbol{\rho}}_{S_T}] \tag{2.15}$$

$$\mathbf{X}_{pq} = [\hat{\mathbf{M}}_{pq1} \hat{\mathbf{M}}_{pq2} \ldots \hat{\mathbf{M}}_{pqS_T}] \tag{2.16}$$

From now on, only derivation for Equation 2.16 is shown, derivations for Equation 2.13 - Equation 2.15 are done in a similar fashion.

The mean of the data is,

$$\overline{\mathbf{X}}_{pq} = \frac{1}{S_T}\sum_i \hat{\mathbf{M}}_{pqi} \tag{2.17}$$

The centralised data is,

$$\mathbf{\Phi}_{pq} = \mathbf{X}_{pq} - \overline{\mathbf{X}}_{pq} \tag{2.18}$$

Let $\mathbf{e}_i$ and λ_i be the eigenvectors and corresponding eigenvalues for the covariance matrix $\mathbf{\Sigma}_{pq} = \mathbf{\Phi}_{pq}\mathbf{\Phi}_{pq}^{T}$. And let $\mathbf{A}$ be a matrix whose rows are formed from the eigenvectors, ordered so that the first row is the eigenvector corresponding to the largest eigenvalue and the last row is the eigenvector corresponding to the smallest eigenvalue. Therefore, the centralized vectors $\mathbf{x}_{pq}$'s can be mapped into vectors denoted by $\mathbf{y}_{pq}$ by the transformation matrix $\mathbf{A}$ as follows,

$$\mathbf{Y}_{pq} = \mathbf{A}\mathbf{\Phi}_{pq} \tag{2.19}$$

The transformation matrix $\mathbf{A}$ is known as the eigenspace transformation matrix (EST).

PCA has the capability of performing data compression by selecting some $k_\lambda \le K_\lambda$ members of eigenvalues that specify some high variance principal components in PCA. To determine the value of k_λ, the number of features to use, the eigenvalues λ_i are sorted in non-increasing order. The residual mean-square error in using $k_\lambda \le K_\lambda$ features is simply the sum of the eigenvalues not used, $\sum_{i=k_\lambda+1}^{K_\lambda}\lambda_i$ [Swets and Weng 1996].

If the percentage $p_\lambda = 5\%$, a good reduction in the number of features is obtained while retaining a large proportion of the variance present in the original feature vector [Jain and Dubes 1988] [Turk and Pentland 1991], thereby losing very little of their original population-capturing power. Based on this principle, a new calculation of k_λ is done in reverse order that is by choosing a fixed percentage $P_\lambda = 5\%$ by Equation 2.20,

$$P_\lambda = \frac{\sum_{i=1}^{k_\lambda} \lambda_i}{\sum_{i=1}^{K_\lambda} \lambda_i} \tag{2.20}$$

2.2.2. Canonical Analysis

After projection into the eigenspace, given C classes having S sequences for each class, the matrix is,

$$\mathbf{Y}_{pq_{ij}} = [\mathbf{y}_{pq_{i1}} \mathbf{y}_{pq_{i2}} \cdots \mathbf{y}_{pq_{iS}}] \tag{2.21}$$

The vectors $\mathbf{y}_{pq_{ij}}$, representing j^{th} sequences in class i are,

$$\mathbf{y}_{pq_{ij}} = [\mathbf{e}_1, \mathbf{e}_2, \ldots, \mathbf{e}_{k_\lambda}] \mathbf{x}_{pq_{ij}} \tag{2.22}$$

The mean vector for the entire set is,

$$\overline{\mathbf{Y}}_{pq} = \frac{1}{S_T} \sum_{i=1}^{C} \sum_{j=1}^{S} \mathbf{y}_{pq_{ij}} \tag{2.23}$$

The mean vector for the i^{th} class is,

$$\overline{\mathbf{y}}_{pq} = \frac{1}{S} \sum_{\mathbf{y}_{pq_{ij}} \in \mathbf{Y}_{pq_i}} \mathbf{y}_{pq_{ij}} \tag{2.24}$$

The within-class and between class matrix are,

$$\mathbf{S}_{\mathrm{w}} = \frac{1}{S_T}\sum_{i=1}^{C}\sum_{\mathbf{y}_{pq_{ij}} \in \mathbf{Y}_{pq_{ij}}} (\mathbf{y}_{pq_{ij}} - \overline{\mathbf{y}}_{pq_{ij}})(\mathbf{y}_{pq_{ij}} - \overline{\mathbf{y}}_{pq_{ij}})^T \tag{2.25}$$

$$\mathbf{S}_{\mathrm{b}} = \frac{1}{S_T}\sum_{i=1}^{C} S(\overline{\mathbf{y}}_{pq} - \overline{\mathbf{Y}}_{pq})(\overline{\mathbf{y}}_{pq} - \overline{\mathbf{Y}}_{pq})^T \tag{2.26}$$

Using the *generalised Fisher linear discriminant function*, to maximise both $\mathbf{S}_{\mathrm{w}}$ and $\mathbf{S}_{\mathrm{b}}$ simultaneously, $J(\mathbf{W})$ has to maximise,

$$J(\mathbf{W}) = \frac{\mathbf{W}^T\mathbf{S}_{\mathrm{b}}\mathbf{W}}{\mathbf{W}^T\mathbf{S}_{\mathrm{w}}\mathbf{W}} \tag{2.27}$$

where, $J(\mathbf{W})$ represents the ratio of within-class to between-class variances.

Let $\mathbf{w}_i$ be the generalised eigenvectors, to maximise $J(\mathbf{W})$ is to differentiate it with respect to $\mathbf{W}$ and represent as a generalised eigenvalue equation,

$$\mathbf{S}_{\mathrm{w}}^{-1}\mathbf{S}_{\mathrm{b}}\mathbf{w}_i = \lambda_i\mathbf{w}_i \tag{2.28}$$

Thus, the eigenvectors are an orthogonal basis that spans a (C-1)-dimensional canonical space and a projection of $\mathbf{y}_{pq}$ into this canonical space becomes another transformed vectors $\mathbf{z}_{pq}$. The $\mathbf{w}_i$'s are also known as the canonical space transformation matrix (CST).

Merging both PCA and CA produce a new equation to apply to test vectors,

$$\mathbf{z}_{pq_{ij}} = [\mathbf{w}_1, \mathbf{w}_2, ..., \mathbf{w}_{k_\lambda}]^T[\mathbf{e}_1, \mathbf{e}_2, ..., \mathbf{e}_{k_\lambda}]^T\mathbf{x}_{pq_{ij}} \tag{2.29}$$

2.3 Conclusions

Gait as defined by Murray [1967] is "a total walking cycle – the action of walking can be thought of as a periodic signal". A gait periodic signal has spatial and temporal characteristics, which are its kinematics traits. In this chapter, angular displacements data and silhouette moments data are

proposed as temporal and spatial representation of gait's data, respectively. Angular displacements data are defined as angle of displacements of the thigh's rotation, the lower leg's rotation, and the foot flexion. The angles are calculated from a set of gathered points, which are manually labelled at each image frames. Silhouette moments data are defined as the Cartesian centralised moments of subject's silhouette at each image frames. They are used, instead of using silhouette itself because a direct computation of silhouette into a descriptor analysis would be tremendous.

This work employs a data-driven approach to analysing gait's data. PCA and CA are statistical-based descriptor analysis suitable for feature extraction process in a data-driven approach system. PCA is a technique of feature extraction for data compression by transforming a dataset into a representation in lower dimensional spaces. CA is a feature extraction technique for data discrimination by minimising the within-scatter variance and maximising the between-scatter variance of the data. In this chapter, the mathematical formulation of PCA and CA are merged so that it can be applied to test data at the classification process.

Chapter 3

GAIT CYCLE EXTRACTION

This chapter describes the gait cycle extraction procedure, which is the pre-processing step in the feature extraction process of the data-driven approach system.

3.1 Introduction

Gait cycle extraction procedure is a pre-processing step in a feature extraction procedure. This step involves a series of two processes: interpolation, which utilises the Support Vector Machines for Regression (SVR) framework and resampling, which defines complete gait cycles to be between zero crossings. It should be noted that in this work regression via SVR is performed not for analysing the data but merely a tool for cycle extraction.

3.2 Problem Definition

Gait data is observational, in which they are finitely sampled and thus the representation signal of its raw data is discrete. Data interpolation is proposed for fitting the best curve that can describe a continuous gait cycle before extraction. Since the cycle needs well-defined start and end points before extraction, by interpolation, the data points within finite intervals of the gait cycle are better estimated. This can reduce the probability of noise effect in the data, allowing more accurate resampling at the start and end points.

Furthermore gait data is high dimensional thus to do calculations in the input space is intractable. Methods based around kernels are chosen for their rigorous formulation and good generalisation [Gunn and Kandola 2001]. Support Vector Machines for Regression (SVR) is an example method, which is based around kernels. The idea of the kernel function is to enable operations to be performed in the input space rather than the potentially high dimensional feature space [Schölkopf 1998].

The support vector machine (SVM) is a universal constructive learning procedure based on statistical learning theory introduced by Vapnik [1995]. In a support vector machine (SVM), the data is mapped into a higher dimensional feature space via a mapping function. The mapping constructs a separating hyperplane with maximum margin in this high dimensional space, which yields a non-linear decision boundary in input space [Schölkopf 2000]. By the use of the kernel function, the separating hyperplane is computed without explicitly carrying out the map in the feature space [Alon et al. 1997].

Likewise the SVMs can also be applied to regression problems by the introduction of an alternative loss function [Smola 1996]. The loss function must be modified to include a distance measure [Vapnik 1995]. Vapnik proposed the ε-insensitive loss function to enable a sparse set of support vectors to be obtained.

Ideally the choice of a set of approximating functions reflects a priori knowledge about the system (unknown dependency) [Schölkopf 1998]. However, in choosing a kernel that best reflects the gait recognition system can also depend on one of these factors: similarity measure for the data, or a (linear) representation of the data, or a hypothesis space for learning [Schölkopf 1998]. The a priori of gait data is its periodicity and continuity. Its data representation is a composition of sinusoidal waves, consistent with earlier 'automated' analysis [Cunado et al. 1999] [Yam et al. 2001] [Yam 2002]. Thus the commonly employed kernel function that can be used to describe the gait data set is the cubic-spline function.

Cubic splines are widely used to fit a smooth continuous function through discrete data [Wolberg and Alfy 2002]. It is used in fields of computer graphics and image processing, where smooth interpolation is essential. Cubic splines use low-order polynomials, which are the piecewise cubic polynomials. The low-order polynomials reduce the computational requirements and numerical instabilities that arise with higher degree curves [Wolberg and Alfy

2002]. Cubic polynomials allow for a curve to pass through two endpoints with specified derivatives at each endpoint. This guarantees continuous first and second derivatives across all polynomials segments, which makes it smooth and attractive for this gait data set.

Resampling is proposed to align the feature vectors for uniformity and invariance due to different start and end points of feature vectors. The numbers of frames captured for a gait cycle are different for each person since each person has different walking speeds. Thus, the sequence lengths for the data (or raw data) are unequal. The sequences can vary from 50 to 77 points for the 10 subjects. Resampling is proposed to be between two consecutive zero crossings for they are the easiest to extract and having the simplest procedure.

Furthermore, resampling can be used to deal with the phase difference in each feature vector. Gait data is a composition of sinusoids with peaks and troughs, which defines the positive and negative phase. The positive and negative phase vectors map to different regions in the feature space, which can affect the recognition performance. In addition, it has been shown that there are significant variations of phase features with individual gaits [Little and Boyd 1998].

Moreover, previous works by other researchers based their gait cycle on heel-strike as a basis for obtaining gait signature. By resampling, this dependency can simultaneously be changed for added flexibility.

3.3 Cycle Extraction Procedure

Each raw data (angular displacements and silhouette moments) of image frames in a gait sequence can be represented by a feature vector using the lexicographic ordering [Jain 1989]. That is each raw data item of each image frames in a sequence is mapped as an item in a column vector, which

represents a corresponding sequence. These sequences then are examined through the cycle extraction procedure.

The cycle extraction procedure begins with the interpolation of the feature vector using the SVR toolbox [Gunn 1998], implemented in Matlab. Interpolation is proposed for fitting the best curve that can describe a continuous cycle before extraction. The cycle extraction procedure ends with the resampling of feature vectors, which is defined to be between two consecutive zero crossings and having similar phase throughout the dataset.

3.3.1 Data Interpolation Formulation

Given vectors of raw data for each sequence of length L,

$$\boldsymbol{\theta} = [\theta_1 \ \theta_2 \ \dots \ \theta_L]^T \ , \ \boldsymbol{\theta} \in [0, 2\pi]^L \tag{3.1}$$

$$\boldsymbol{\phi} = [\phi_1 \ \phi_2 \ \dots \ \phi_L]^T \ , \ \boldsymbol{\phi} \in [0, 2\pi]^L \tag{3.2}$$

$$\boldsymbol{\rho} = [\rho_1 \ \rho_2 \ \dots \ \rho_L]^T \ , \ \boldsymbol{\rho} \in [0, 2\pi]^L \tag{3.3}$$

$$\mathbf{M}_{pq} = [\mu_{pq_1} \mu_{pq_2} \dots \mu_{pq_L}]^T \ , \ \mathbf{M}_{pq} \in \Re^L \tag{3.4}$$

where $\theta_i = \theta(t_i)$, $\phi_i = \phi(t_i)$, and $\rho_i = \rho(t_i)$ are the angular displacements of the thigh, the leg, and the foot at time t_i, respectively and $\mu_{pq_i} = \mu_{pq}(t_i)$ are the central moment of order $(p+q)$ for each silhouette at time t_i.

The interpolation estimate in an SVM for Equation 3.4 is of the form,

$$\hat{\mu}_{pq}(t) = \sum_{i=1}^{L} \alpha_i K(t_i, t) \tag{3.5}$$

where, $\alpha_i \in \Re$ are the support vectors, $K(t_i, t)$ is a kernel function and t_i are the training input space points.

The preferred kernel function is the cubic spline,

$$K(t_i,t)=1+t_i t+\frac{1}{2}t_i t\min(t_i,t)-\frac{1}{6}(\min(t_i,t))^3 \tag{3.6}$$

This estimate applies to angular displacements of thigh (θ), leg (ϕ), and foot (ρ) as well.

The resampled vector estimate is of length r,

$$\hat{\boldsymbol{\theta}}=\left[\theta_1\ \theta_2\ \ldots\ \theta_r\right]^T\ ,\quad \boldsymbol{\theta}\in[0,2\pi]^r \tag{3.7}$$

$$\hat{\boldsymbol{\phi}}=\left[\phi_1\ \phi_2\ \ldots\ \phi_r\right]^T\ ,\quad \boldsymbol{\phi}\in[0,2\pi]^r \tag{3.8}$$

$$\hat{\boldsymbol{\rho}}=\left[\rho_1\ \rho_2\ \ldots\ \rho_r\right]^T\ ,\quad \boldsymbol{\rho}\in[0,2\pi]^r \tag{3.9}$$

$$\hat{\mathbf{M}}_{pq}=[\mu_{pq_1}\mu_{pq_2}\ldots\mu_{pq_r}],\quad \mathbf{M}_{pq}\in\Re^r \tag{3.10}$$

3.3.2 Resampling Procedure

The resampling procedure discussion is based on the angular displacements data specifically on the limb inclination of the thigh since the thigh angular displacements was the first analysis attempted. There are three possible methods to base the resampling on: between two consecutive maximum points, minimum points, or zero crossings.

Resampling between Consecutive Maximum Points. The initial plan was to resample at the first and the third extreme maximum points since the inclination of the thigh is maximum at these points during a gait cycle. However there is the sudden decrease in angle value around the principal maximum peak for the hip angle data. Referring to Figure 3.1, there are inflexion points around the maximum peak. This decrease in angle value in

Figure 3.1(b) might be due to the shifting of the body weight onto the front foot. This can be seen in Figure 3.1(a) when the front leg is just about to strike the floor. Heel strike occurs in the next frame; simultaneously the body weight starts to shift its load onto that foot. At Figure 3.1(c), when the front foot is already flat, the back foot still flexes at its original position but the hip position already moves forward creating a larger inclination between the thigh and the vertical. Furthermore, according to Perry [1992], the body weight shifts from one leg to another when both feet are in contact with the ground[2]. This condition occurs at maximum peaks of all sequences for the hip angle, thus resampling cannot be based on maximum peaks.

Resampling between Consecutive Minimum Points. Since maximum points are difficult to extract, minimum points might be a possibility. However, there is a problem with the video itself. The image files that were extracted start at heel strike and end at heel strike of the same leg. There are no image files before and after that heel strike. Hence, there are some sequences that do not have a complete cycle based on minimum points.

Resampling between Consecutive Zero Crossings. Therefore, the task is changed to extraction of a gait cycle at zero crossing. Other than being simpler, zero crossing extraction can be a generic cycle extraction technique for extending to other input data types thus, making the cycle extraction procedure more robust to other gait data types.

Also the difference in phase can affect the mapping of data in feature space. It has been shown that the phase features of individual gaits have significant

[2] As the body moves forward, one limb serves as a mobile source of support while the other limb advances itself to a new support site. Then the limbs reverse their roles. For the transfer of body weight from one limb to the other, both feet are in contact with the ground. This series of events is repeated by each limb with reciprocal timing until the person's destination is reached [Perry 1992].

variation [Little and Boyd 1998]. Cycle extraction of a sequence with positive phase will be mapped onto a positive region of the feature space and vice versa. This is shown in Figure 3.2 whereby the positive phase dataset are mapped on the positive side of the feature vector and the negative phase dataset are mapped on the opposite side. Thus, the extraction is chosen to having similar phase direction for all sequences of gait data types.

3.4 The Implementation

The implementation of the cycle extraction algorithm is done automatically in Matlab using a Pentium III 700MHz processor. The sampling rate is chosen to be 30. The phase of the feature vector is set to positive.

Cycle Extraction Algorithm

1. Gather θ_i, ϕ_i, ρ_i, and μ_{pq_i} for each sequences.
2. Apply SVR function of Equation 3.5.
3. Equate $\hat{\theta}_i$, $\hat{\phi}_i$, $\hat{\rho}_i$, and $\hat{\mu}_{pq_i}$ to zero.
4. Compute the roots of the polynomial whose coefficients are the elements of the vector $\hat{\theta}_i$, $\hat{\phi}_i$, $\hat{\rho}_i$, and $\hat{\mu}_{pq_i}$.
5. Take two consecutive zero crossings, which define complete cycle.
6. Evaluate the phase of the feature vector.
7. If phase evaluation is negative, repeat step 5. Else go to step 8.
8. Resample the vector estimate at sampling rate, $n = 30$.
9. Save the resampled vector estimate.

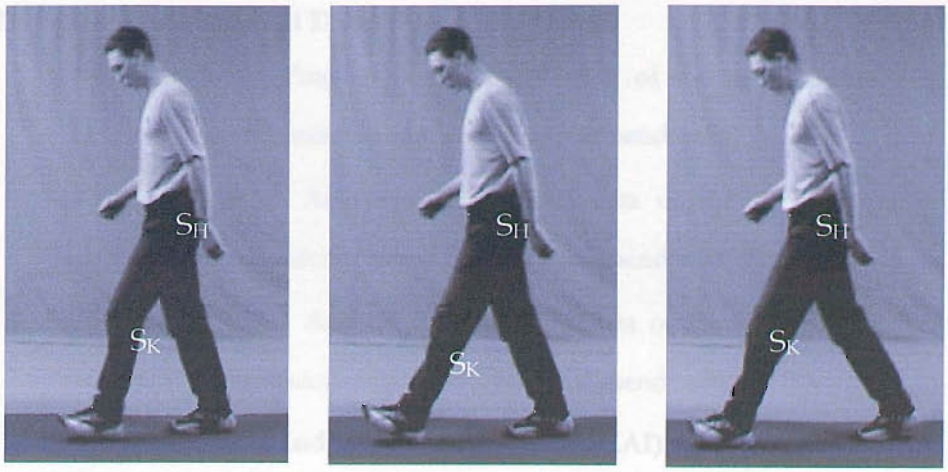

(a) Frame 32, $\theta = 21.3°$ (b) Frame 34, $\theta = 18.4°$ (c) Frame 36, $\theta = 19.8°$

Figure 3.1: Inflexion points on an example subject.

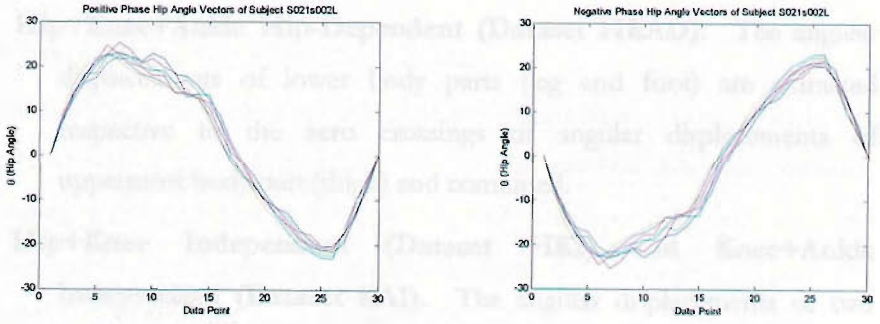

(a) Positive phase (b) Negative phase

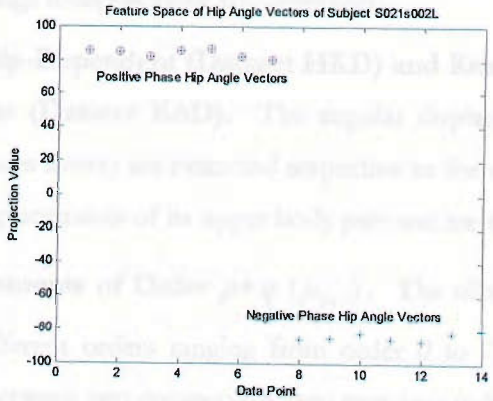

Figure 3.2: Feature space mapping of feature vectors with different phase.

Definitions of Extracted Data

Hip Angle (θ_i). Angular displacements data of the thigh extracted between two consecutive zero crossings independently.

Knee Angle (ϕ_i). Angular displacements data of the leg extracted between two consecutive zero crossings independently.

Ankle Angle (ρ_i). Angular displacements data of the foot extracted between two consecutive zero crossings independently.

Hip+Knee+Ankle Independent (Dataset HKAI). The three angular displacements data, each has been extracted between two consecutive zero crossings independently and combined by stacking each angular displacements onto a column feature vector with the uppermost body part on top.

Hip+Knee+Ankle Hip-Dependent (Dataset HKAD). The angular displacements of lower body parts (leg and foot) are extracted respective to the zero crossings of angular displacements of uppermost body part (thigh) and combined.

Hip+Knee Independent (Dataset HKI) and Knee+Ankle Independent (Dataset KAI). The angular displacements of two body parts data, each has been extracted between two consecutive zero crossings independently and combined.

Hip+Knee Hip-Dependent (Dataset HKD) and Knee+Ankle Knee-Dependent (Dataset KAD). The angular displacements of body part (the ones lower) are extracted respective to the zero crossings of angular displacements of its upper body part and are combined.

Silhouette Moments of Order $p+q$ (μ_{pq_i}). The silhouette moments data of different orders ranging from order *0* to *7*, each has been extracted between two consecutive zero crossings independently.

Silhouette Moments upto Order $p+q$. The silhouette moments data of different orders ranging from *0* to 7, each has been extracted

between two consecutive zero crossings and combined according to the defined upto-order by stacking each order (with the lowest order on the top) onto a column feature vector.

Note that the selection of the combined independently and dependently extracted data is formulated for analysing the affect of temporal changes. That is whenever data are independently extracted; they have different time frames that associate with the zero crossings.

3.5 Description of Findings

All resulting curves in the figures show: the plus (+) in the circles are the support vectors, which correspond to the discrete raw data in the sequence. The bold lines are the resulting interpolated curve from the SVR plotting tool. The sampling rate is set at 30.

3.5.1 Angular Displacements Data

Angular displacements data are values of limb inclination of thigh and leg, and values of flexion of the foot, which are manually labeled. They are displayed in Figure 3.3, Figure 3.4, and Figure 3.5, with corresponding frames of gait motion at several points of interest, namely the maximum points, the minimum points, and the zero crossings. These figures plot at least two complete gait cycles.

Figure 3.3 shows the plot of thigh angular displacements for subject S013s00L, which is referred throughout this thesis. There are six frames of interest: frame 10, frame 15, frame 23, frame 34, frame 36, and frame 54. Frame 10 is the frame where the subject is at heel-strike for the first complete gait cycle, which started with the left leg. The angle is at its maximum, consistent with Murray's work, which has been defined in section 2.1. Frame 15 is the frame when both legs intercepts, which happen during leg swing. Thus the angle value is almost 0 degree. The minimum point is at Frame 23, where at this time the right leg is at its heel strike. It is a negative value because the positive hip angle has been defined in section 2.3.1 to be the

angle in the direction of the walking. Between frame 34 and frame 36 is the occurrence of the inflexion points, which has been discussed in section on resampling procedure (section 3.3.2). Frame 54 is the frame where the subject leaves the view of the camera. It is interesting to note that at this frame, the view of the leg slightly moves. That is the view of the leg is not normal to the view of the camera. This phenomenon is discussed in literatures on view-invariant gait recognition [Johnson and Bobick 2001] [Shaknarovich 2001] [Abdelkader 2002a].

The regressed curve for knee angle is shown in Figure 3.4. Similar to hip angle curve, the maximum point at frame 7 corresponds to the leg at heel-strike. Frame 16 and frame 31 are frames when the leg interception occurs. However, at frame 27, the minimum point does not refer to heel-strike, but corresponds to the leg movement in the swing phase; in this case the left leg is in the swing phase because the right leg starts with the heel-strike. Thus, the maximum opening of legs can occur during heel strike and during the start of the swing phase.

The ankle angle is the foot flexion during walking. Its value is positive almost all the time during walking except at heel-strike in Figure 3.5. This can be viewed in frame 7. All other frames of interest have positive angle values except frame 7, whereby the foot flexes to allow for the heel to strike the floor. Frame 26 is the peak of the feature vector, which refers to the end of the stance phase and the start of the swing phase for the left leg.

Figure 3.6 and Figure 3.7 shows the plots of feature vectors for dependently and independently extracted data. The choice for combining feature vectors by dependently extracted and independently extracted is to investigate the affect of temporal difference in feature vectors. Figure 3.6 shows the independently extracted combination feature vectors (dataset HKAI). Figure 3.7 shows the dependently extracted combination feature vectors (dataset HKAD). Feature vectors in Figure 3.6 for the hip, knee, and ankle angles are

zero at the start and end points, which indicates they are independently extracted. The temporal information is different for each angular displacement but the start and end points have similar angular values. Figure 3.7 indicates that the hip, knee, and ankle angles are dependently extracted since the time of start and end points is zero but the respective angular values are not. Therefore, the affect of the difference in temporal information can also be analysed.

It is important to note that the attire a person wears can affect the labeling of the data. Some subjects wear their shirts tucked into their trousers, which makes the determination of the hip points simpler, but some do not. The labeling for the knee and ankle points is affected by the type of trousers the person wears that is a person wearing a knee-length trousers versus long trousers and tight fitting trousers versus loose fitting trousers or boot-cut trousers. It is also difficult to determine the labeling points of the toes especially for subjects wearing jogging shoes because the outer covering of the shoes is thicker than those of sandals. This can be viewed in Figure 3.8.

In addition, the arm does occlude the view of the hip points for some subjects at certain points. When such a case occurs the determination of the labeling point at the hip is guessed but with comparison to the immediate previous and later frames in the sequence. These uncertainties in determination of the labeling points can be a potential noise for the feature vectors since a change of one pixel in the x or y coordinates is a difference of about 18° in angular values[3]. This value can be significant if the change of the pixel location is more than one.

---

[3] This is measured as below:

$$\tan 45^\circ = \frac{|1|}{|1|}$$

if pixel difference increase by 1 in either x or y coordinates,

$$|\theta - 45^\circ| = \left|\tan^{-1}\frac{|2|}{|1|} - \tan^{-1}\frac{|1|}{|1|}\right| = \left|\tan^{-1}\frac{|1|}{|2|} - \tan^{-1}\frac{|1|}{|1|}\right| = 18^\circ$$

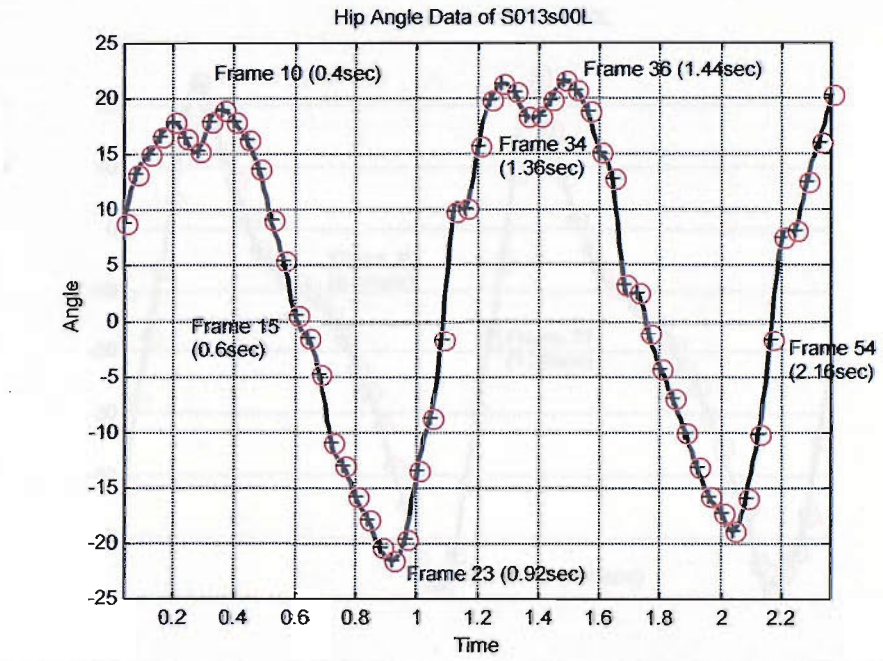

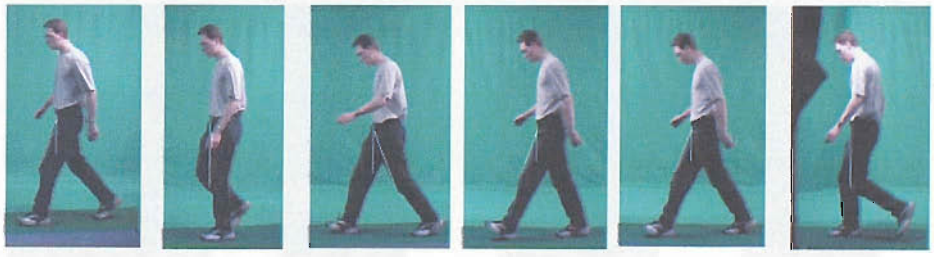

Frame 10 Frame 15 Frame 23 Frame 34 Frame 36 Frame 54

Figure 3.3: An example SVR curve for thigh angular displacements with corresponding frames showing the gait motion.

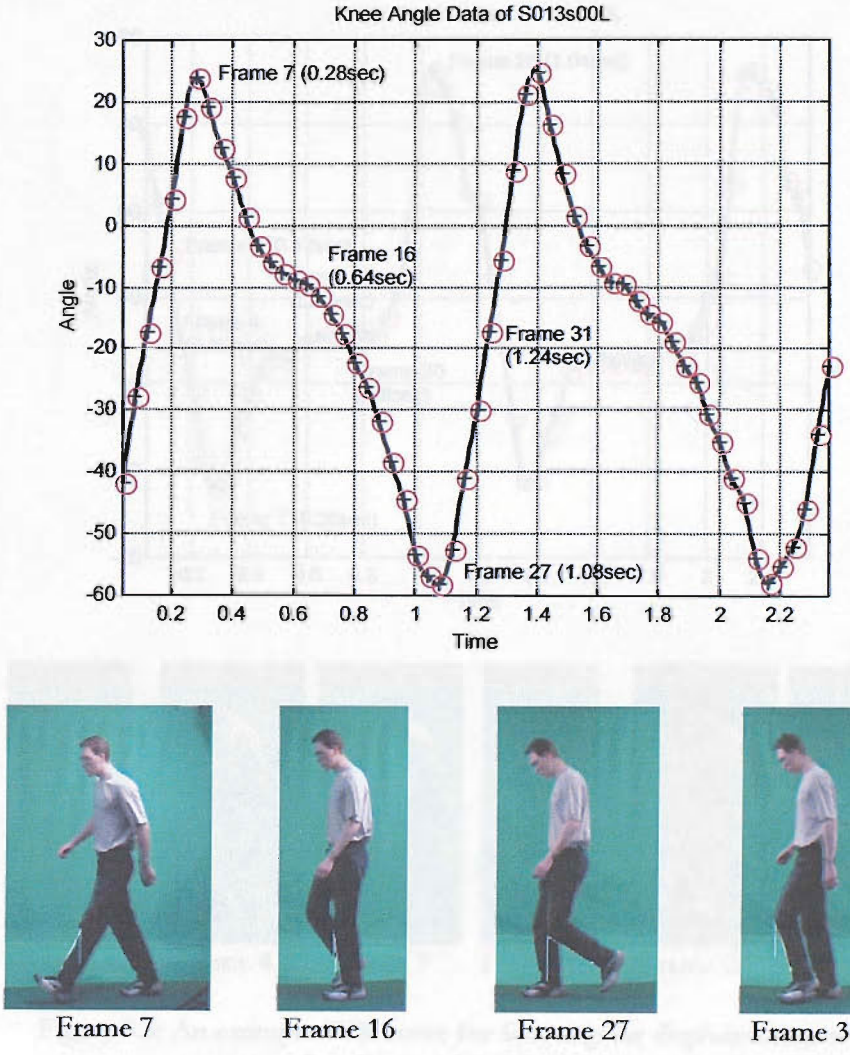

Figure 3.4: An example SVR curve for leg angular displacements with corresponding frames showing the gait motion.

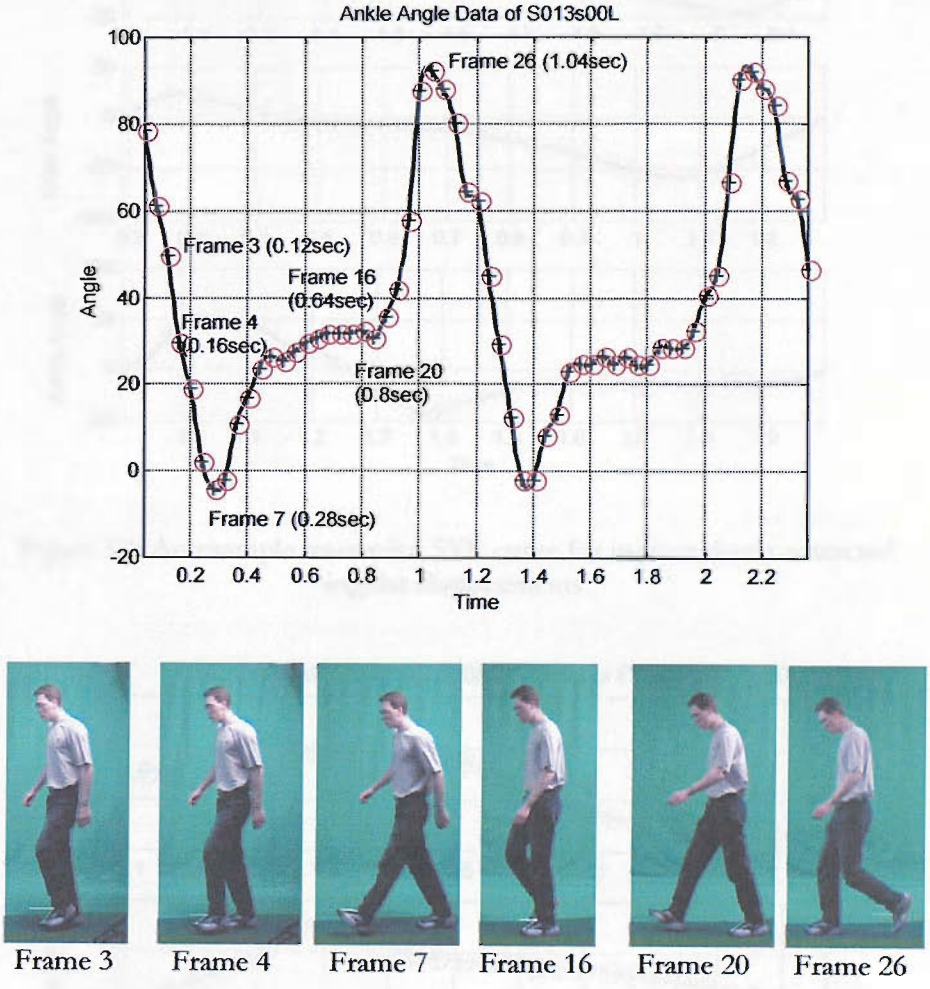

Figure 3.5: An example SVR curve for foot angular displacements with corresponding frames showing the gait motion.

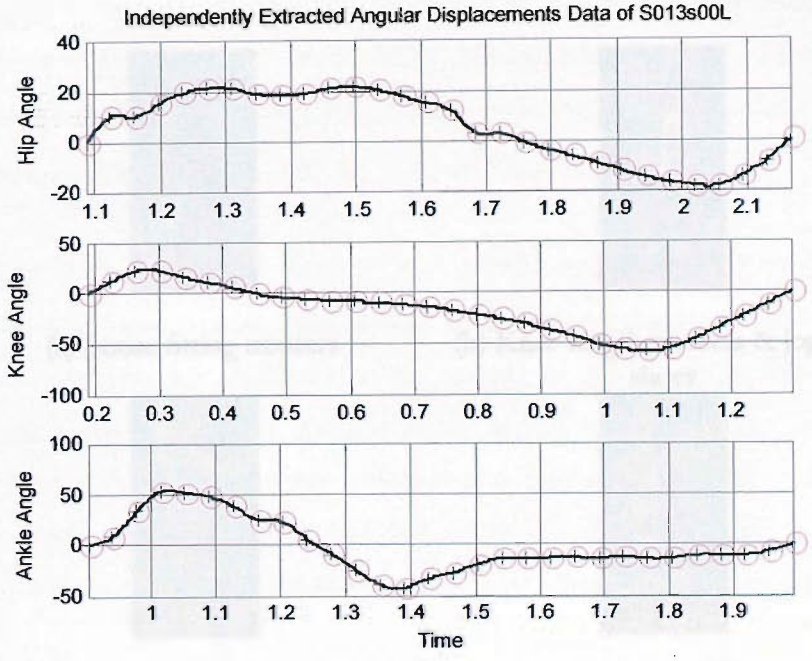

Figure 3.6: An example resampled SVR curve for independently extracted angular displacements.

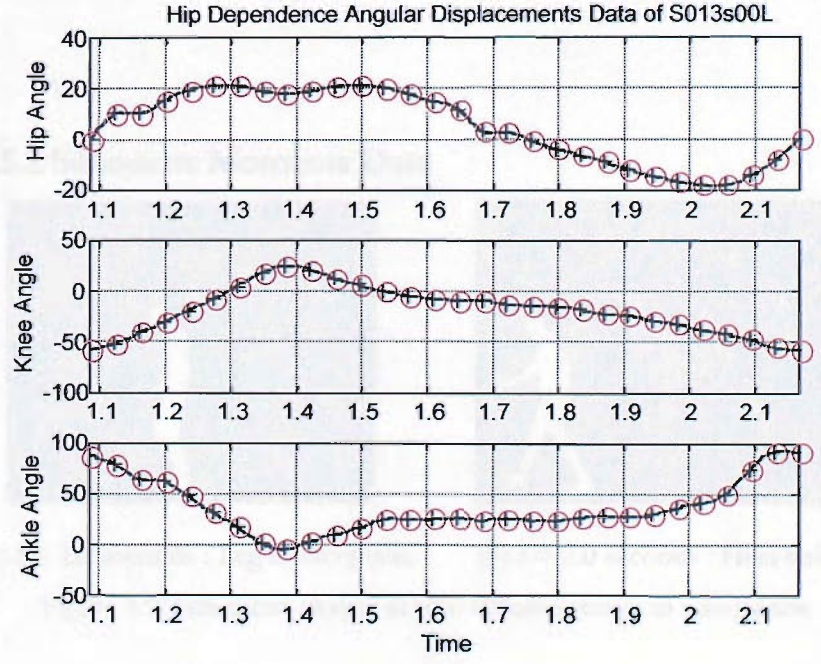

Figure 3.7: An example resampled SVR curve for hip dependence angular displacements.

(a) Loose fitting trousers

(b) Knee-length trousers & jogging shoes

(c) Tight fitting trousers & tucked-in shirt

(d) Boot-cut trousers & sandals

Figure 3.8: Difference in attire for different subjects.

3.5.2 Silhouette Moments Data

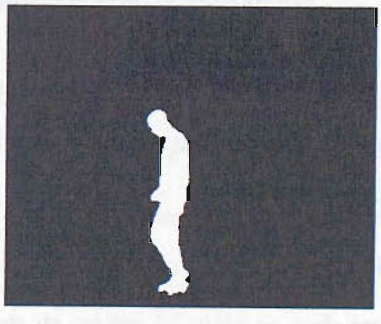

(a) t = 1.2 seconds : Leg interception

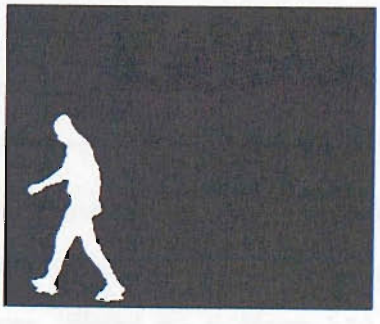

(b) t = 2.0 seconds : Heel strike

Figure 3.9: Silhouette shapes at two different times in a sequence.

Figure 3.10 (a)-(f) show some examples of the moment vectors after regression for one of the subject in the gait silhouette database. Note that moments of 0^{th} and 1^{st} order, (m_{00}, m_{10}, m_{01}) are not calculated using central moments (Equation 2.8) since $m_{00} = \mu_{00}$ and $\mu_{01} = \mu_{10} = 0$.

Figure 3.10 (a) displays moment m_{00}, which represents the area or the number of pixels that an image frame has in the gait sequence. The result is consistent with our intuition that the number of pixels changes with each image frame. That is at different image frames there are larger areas of silhouette shapes, which can correspond to the subject at heel strike (at maximum angle) for example, and there are smaller areas of silhouette shapes, which can correspond to the subject at leg interception (at minimum angle).

Figure 3.10 (b) and (c) correspond to the sequences of horizontal and vertical centre of mass for the subject. In Figure 3.10 (b), the horizontal direction centroid decreases in time since it represents the x-coordinates of the silhouette shapes, which changes from coordinate 720 to 0 if the subject walks from right to left and vice versa. In Figure 3.10 (c), the vertical direction centroid represents changes to the y-coordinates' centre of the silhouette shapes for that sequence, in which it moves with the motion of a walking person at each frame.

Figure 3.10 (d), (e), and (f) show the sequences of second-order central moments, μ_{11}, μ_{20}, and μ_{02} respectively. From the definitions stated in section 2.3.2, μ_{20} in Figure 3.10 (e) is the horizontal direction variance, which correspond to the displacements of the y-coordinates for the silhouette shape from its centre of mass at each image frames. Whilst μ_{02} in Figure 3.10 (f) refers to the vertical direction variance, which corresponds to the displacements of the x-coordinates for the silhouette shape from its centre of mass. These variances are consistent with the area plot in Figure 3.10 (a), where smaller areas, which have smaller width and/or height shapes have low

displacement values from its centroid and vice versa. This can be seen for example at time t = 1.2 seconds (Figure 3.9 (a)), for at this time the legs are intercepting; the angle is minimum and the silhouette shape is small. And at time t = 2.0 seconds (Figure 3.9 (b)), the subject is at heel strike and the displacement value is high.

Figure 3.11 shows comparison plots between silhouette moments data of left and right sequences. It can be seen that the plots of the left sequences and the right sequences are symmetrical around the y-axis. This happens due to the horizontal movement of the x-coordinates, which moves with the silhouette. Moments calculations involve the x and y coordinates of silhouettes, thus the changes of x-coordinates either ascending or descending affect the silhouette moments.

Moreover, the scale of the moments values, which has values as high as the power of nine for moments order 3 and definitely it is higher for higher moments order. This difference in the range of values can affect the mapping into feature space, in which higher order moments will dominate the projection. Thus, some form of normalisation is needed to overcome this.

Assuming that the data is normally distributed, the normalisation method is proposed to be the standard z score, which is a standard measurement in statistic. Each data is first subtracted from the mean of the dataset and then divided by the standard deviation of the dataset.

From Figure 3.10 and 3.11, it can be seen that whenever the moments order goes up, a gait cycle is difficult to define, which can make the determination of the zero crossings difficult. Therefore, for a silhouette dataset, feature vectors of moments order variations are dependently extracted based on zero crossings of feature vectors with a comprehensible cycle. For example, in Figure 3.11, the feature vectors for μ_{21} can be a good basis for cycle extraction of other variations.

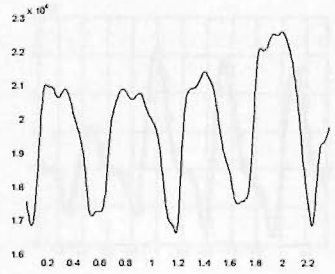

(a) m_{00} : Area

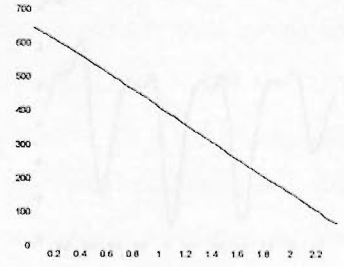

(b) m_{10} : Horizontal Direction Centroid

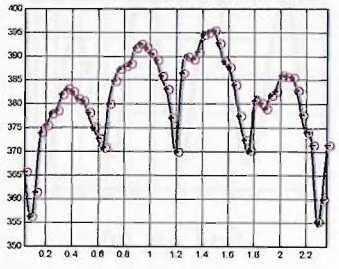

(c) m_{01} : Vertical Direction Centroid

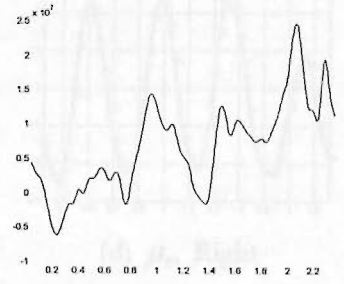

(d) μ_{11}

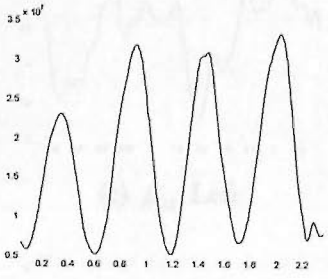

(e) μ_{20} : Horizontal Direction Variance

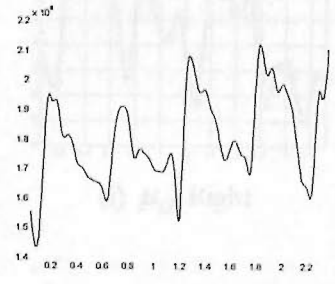

(f) μ_{02} : Vertical Direction Variance

Figure 3.10: Examples of low-order silhouette moments data for a subject walking from right to left.

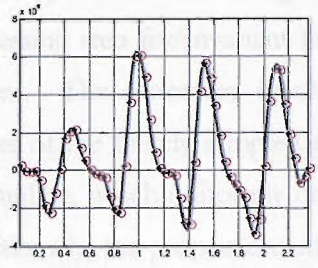

(a) μ_{30} Left

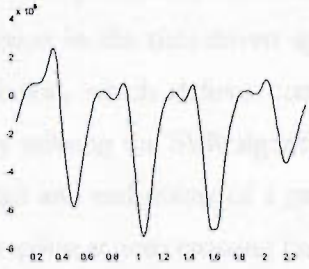

(b) μ_{30} Right

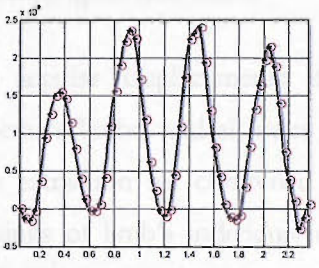

(c) μ_{21} Left

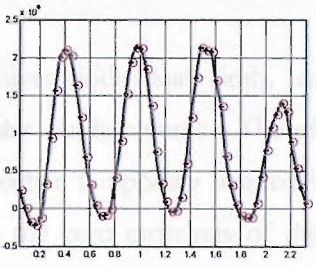

(d) μ_{21} Right

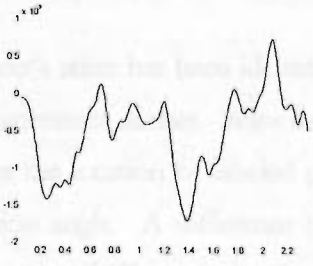

(e) μ_{12} Left

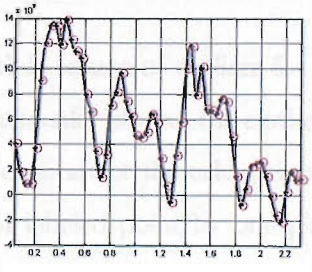

(f) μ_{12} Right

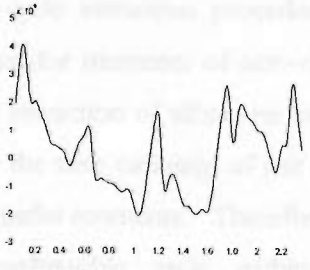

(e) μ_{03} Left

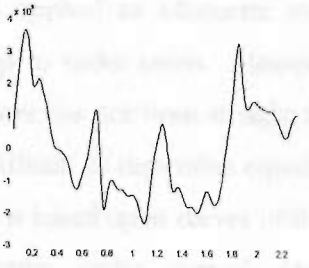

(f) μ_{03} Right

Figure 3.11: Comparison between silhouette moments of order 3 for left and right sequences of a subject.

3.6 Conclusions

This chapter describes the gait cycle extraction procedure, which is a pre-processing step for invariant feature extraction in the data-driven approach system. The procedure involves interpolation, which defines continuous curves of the finitely sampled gait's data by utilising the SVR algorithm and resampling, which uniformly defines the start and end points of a gait cycle. Additionally, the proposed method of resampling at zero crossing has added flexibility to the process of defining a gait cycle, which previously has been depended upon heel-strike.

The angular displacements dataset involves individual limb, any two immediate limbs, and all three limbs angular displacements. Therefore the cycle extraction for combined dataset is either temporally aligned by zero crossings of limb's individual cycle or by the zero crossings of the upper limb's cycle within the combination. This alignment can investigate the affect of differing temporal information for combined dataset.

Subject's attire has been identified as a possible source of outliers for angular displacements dataset. Since the dataset is manually labeled, the clothes could affect the location of labeled points and hence affect the calculation of the rotation angle. A difference of location of labeled point by one pixel is a difference of 18° in angular displacements.

The cycle extraction procedure has been applied to silhouette moments dataset for moments of zero-order until up to order seven. However, the cycle extraction of silhouette moments dataset has not been straight forward since the zero crossings of gait curves are difficult to determine especially for high order moments. Therefore extraction is based upon curves of the most comprehensible cycle within the moments order curves' variations. Moreover, the dataset involves data of large scale moments. Thus, a z score normalisation is applied to the dataset before PCA and CA analysis.

Chapter 4

EXPERIMENTAL RESULTS

4.1 Experimental Design

For recognition purposes, the feature dataset after cycle extraction will be divided into test set and training set. The test set will be taken from one sequence of one subject, and the remainder will be treated as the training set. First, the training data is applied to the PCA+CA algorithm. This will set the EST and CST matrices of the PCA+CA algorithm, which will then be used for projection of the test set into the feature space. In this feature space, the classifier, which is the *k*-nearest neighbour, is applied to calculate the recognition rate. The recognition rate is found at any instances that the test set is correctly identified as belonging to the correct class.

A leave-one-out cross-validation process is applied for each sequence for all subjects, in that each sequence will become a test set at one experimental instance or another. There are 140 experimental instances, which correspond to the total number of sequences the dataset has. At any experimental instances, there will be 139 total sequences for training set and only one sequence is selected as a test set. A counter is used to count at any instances the nearest-neighbour classifier correctly identifies the test set. With this cross-validation procedure, the recognition rate is taken as the average of all correctly identified instances throughout all classes. The experiment is designed this way to test the effectiveness of all those feature vectors by directly testing the recognition rates that occurred at each experimental instance. Also, it is hoped that the computed recognition rate will be an unbiased estimate of the true recognition rate.

It should be noted that the work in this thesis is not on classifier design; hence *k*-nearest neighbour classifier is selected for its simplicity. The distance measure is the Euclidean distance.

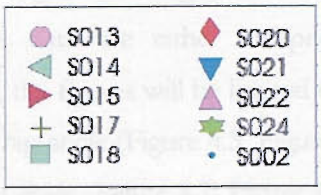

Figure 4.1: Legend used in feature spaces; S013 represents subject 013.

4.2 Angular Displacements Data

Table 4.1: Average Correct Classification of Angular Displacements Data

How Data is Combined	Angles Used [Dataset Name]	*k = 1*	*k = 3*	*k = 5*
Independent Extraction	Hip, Knee, & Ankle [Dataset HKAI]	95.0 %	94.3 %	91.4 %
	Hip & Knee [Dataset HKI]	88.6 %	85.7 %	79.3 %
	Knee & Ankle [Dataset KAI]	79.3 %	77.9 %	68.6 %
Extraction based on Hip	Hip, Knee, & Ankle [Dataset HKAD]	**97.9 %**	**97.9 %**	**95.0 %**
	Hip & Knee [Dataset HKD]	92.1 %	91.4 %	84.3 %
Extraction based on Knee	Knee & Ankle [Dataset KAD]	84.3 %	77.1 %	68.6 %
Individual Extraction	Hip	79.3 %	76.4%	65.0 %
	Knee	70.7 %	66.4 %	65.7 %
	Ankle	62.9 %	63.6 %	45.7 %

Experiments on angular displacements data include the experiments of individual hip angle, knee angle, ankle angle, and combination of these angles. The combination angles data are either independently or dependently extracted. In this section, the figures will be limited to the three basic angular displacements, which are hip angle (Figure 4.3, Figure 4.4), knee angle (Figure 4.5, Figure 4.6), and ankle angle (Figure 4.7, Figure 4.8). The information on the basic angular displacements would be used for estimating the performance of the combined angular displacements.

Figure 4.3, Figure 4.5, and Figure 4.7 shows the pareto[4] plots of the eigenvalues, which explain the percentage variability in the distribution of the eigenvalues. These eigenvalues are from the covariance matrix of the hip, knee, and ankle angle calculated using PCA. Based on Equation 2.20, the transformed features data are truncated to retain 95% of its total maximum variance. In Figure 4.3, 10 eigenvalues account for 95% of the variance in the hip angle data. In fact the first four of these eigenvalues explain roughly three-quarters of the total variability of the hip angle data. Thus, when performing discrimination analysis on the data set, accordingly they cluster quite well. This can be seen in Figure 4.4, where there are few overlaps in the data. The average recognition rate is found to be about 79%.

For the knee angle data set, only six eigenvalues explain the 95% of the total data set variability, which has been based on Equation 2.20. The first three eigenvalues dominate the total variance accountability in the data set. This can be seen in Figure 4.5. The resultant canonical space is in Figure 4.6. However, the classes of each subject in the knee angle data have more

[4] Pareto chart shows the most frequently occurring factors. It is named after Vilfredo Pareto (1848-1923) in Italy. His observations on wealth distribution on the Italian population were further strengthened by Juran in 1960, which formulated the Pareto Principle, which states that, "Not all of the causes of a particular phenomenon occur with the same frequency or with the same impact" [Tham 1997]. Pareto plot is well suited to highlight the percentage of variability contribution of each eigenvalue. The bar-plots show the percentage contribution of each eigenvalue to total number of eigenvalues. The line plot is a cumulative line when each of these eigenvalues is sequentially summed.

overlaps in comparison to the data of thigh displacements. This explains the lower recognition rate on knee angle data, which is about 70%.

Figure 4.7 is the pareto plot of the eigenvalues in the ankle angle. About two-thirds of the total variability in the data set is explained by the first three eigenvalues. Its feature space in Figure 4.8 shows clusters of overlaps in the middle of the feature space, thus the average recognition rate is about 63%.

From here, it is apparent that the upper leg data set produces higher average recognition rate than the lower leg data set. This may indicate that the upper leg, which is the hip angle, accounts for the most variations in walking patterns. However, to recognise a person better, a combined angle data set may be used. They can be independently extracted and dependently extracted but both give a higher recognition rate than using the angular data sets independently. All recognition rates for combined angles dataset are higher than the individual angular dataset. This can be seen in Table 4.1.

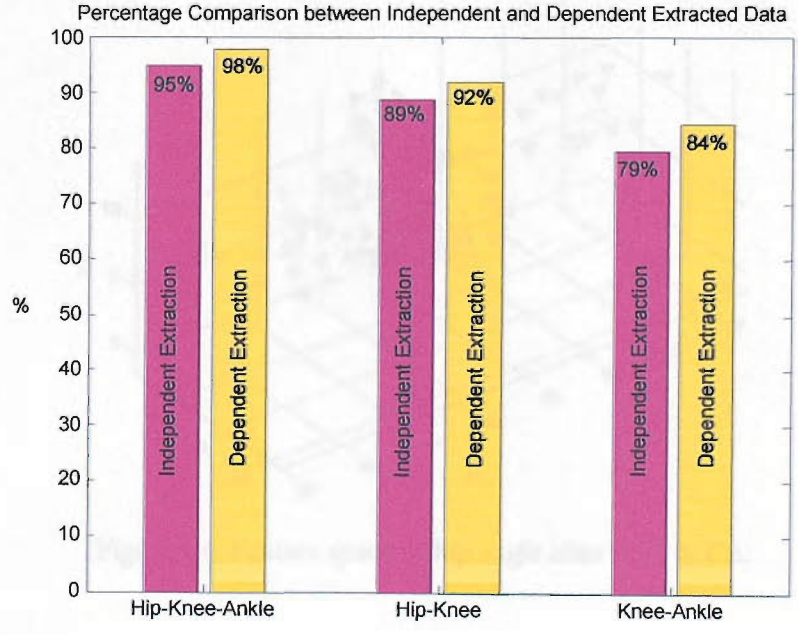

Figure 4.2: Percentage comparison between combined angular displacement datasets.

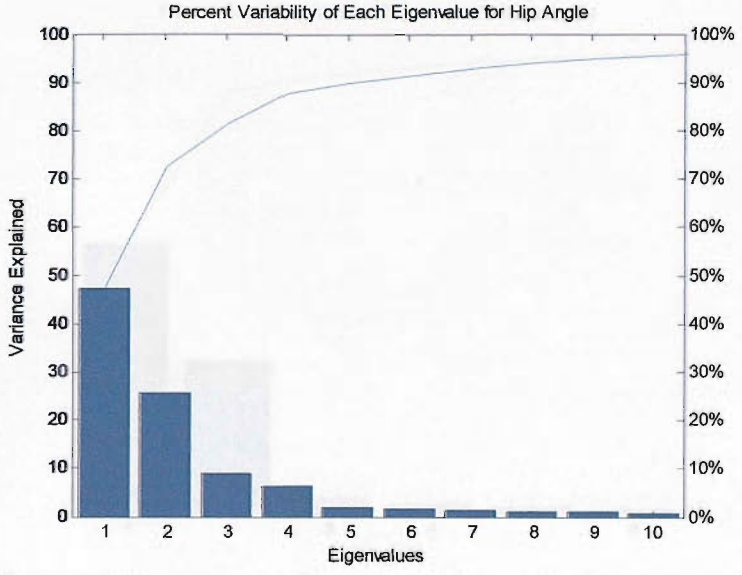

Figure 4.3: Percent variability of each eigenvalue of hip angle.

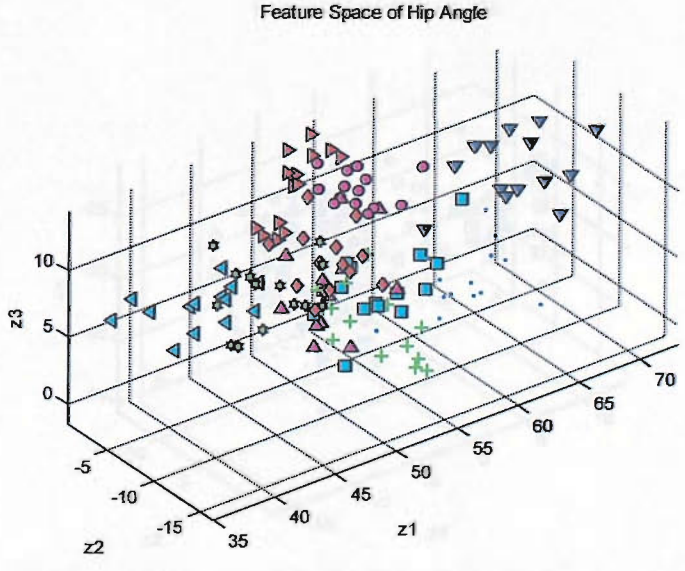

Figure 4.4: Feature space of hip angle after PCA & CA.

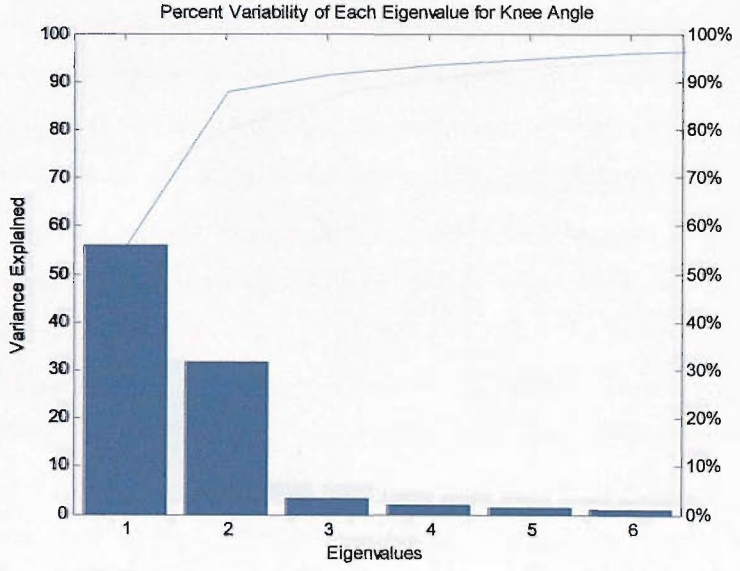

Figure 4.5: Percent variability of each eigenvalue of knee angle.

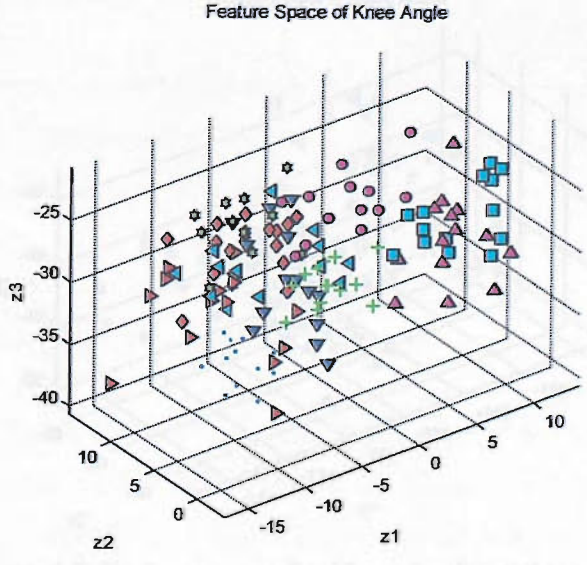

Figure 4.6: Feature space of knee angle after PCA & CA.

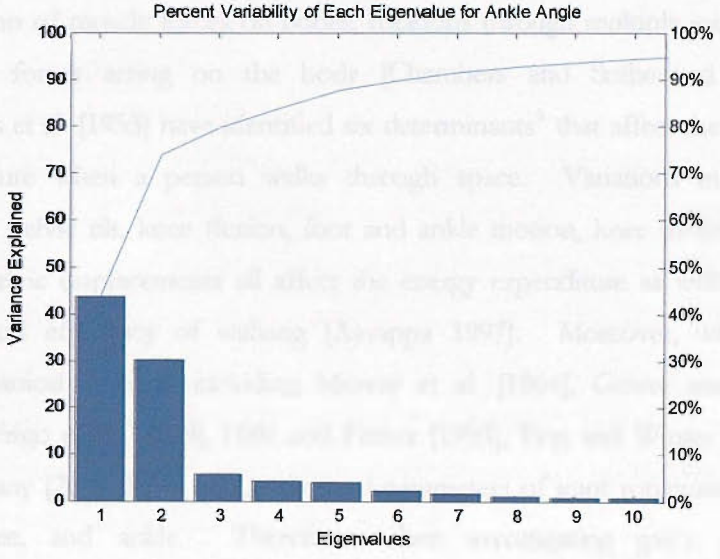

Figure 4.7: Percent variability of each eigenvalue of ankle angle.

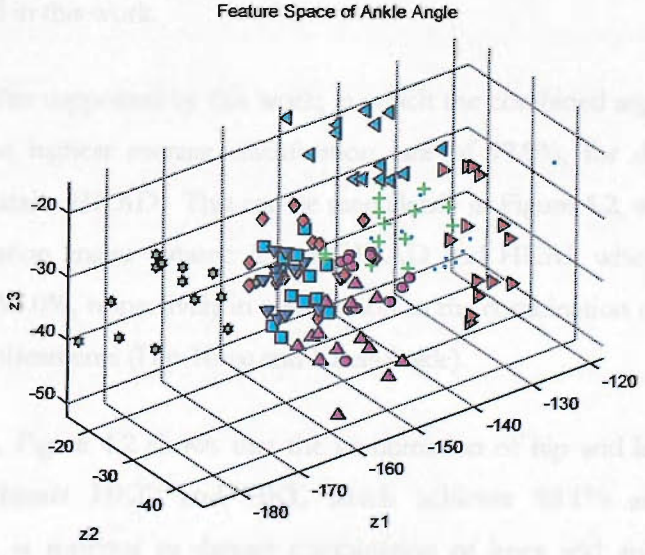

Figure 4.8: Feature space of ankle angle after PCA & CA.

In Section 2.1, gait is considered by Murray [1967] to be a total walking cycle. Walking being the body's natural means of locomotion, involves the complex interaction of muscle forces on bones, rotations through multiple joints and physical forces acting on the body [Chambers and Sutherland 2002]. Saunders et al. [1953] have identified six determinants[5] that affect the energy expenditure when a person walks through space. Variations in pelvic rotation, pelvic tilt, knee flexion, foot and ankle motion, knee motion, and lateral pelvic displacements all affect the energy expenditure as well as the mechanical efficiency of walking [Ayyappa 1997]. Moreover, work on biomechanical research including Murray et al. [1964], Grieve and Gear [1966], Frigo et al. [1989], Hills and Parker [1993], Eng and Winter [1995], and Lakany [2000] have frequently used parameters of joint rotations of the hip, knee, and ankle. Therefore, when investigating gait's angular displacements, it is natural to consider all possible angular displacements. Thus, the choice for analysis of combined angular displacements, which is investigated in this work.

This is further supported by this work, in which the combined angles dataset achieves the highest average classification rate of 97.9%, for dependently extracted dataset HKAD. This can be seen clearly in Figure 4.2, whereby for all combination angles dataset: dataset HKAD and HKAI, which achieves 97.9% and 95.0%, respectively in comparison to the combination of only two angular displacements (Hip-Knee and Knee-Ankle).

In addition, Figure 4.2 shows that the combination of hip and knee angles dataset: dataset HKD and HKI, which achieves 92.1% and 88.6%, respectively is superior to dataset combination of knee and ankle angles: dataset KAD and KAI, which achieves only 84.3% and 79.3%, respectively.

[5] The authors began by assuming that a gait pattern is most efficient when it minimises vertical and lateral excursions in the body's centre of gravity (COG). They identified those features of the movement pattern that minimise these COG excursions. They suggested that these features determine whether a movement pattern is normal or pathological [Thomson 1998].

In fact, the average recognition rate is higher when the hip angle is involved in the combination datasets. This proves that the hip angle does account for the most variation and thus contributes to the increase of correct classification rate in the dataset.

Furthermore Cutting and Profitt [1981] suggested that gender may be identified indirectly through the determination of the 'centre of moment' of a walker. The centre of moment is 'the point about which all movement, in all body parts, has regular geometric relations' [Cutting and Profitt 1981]. The study measures the differences in shoulder and hip widths to recognise between men and women. The hip, which is the body part nearest to this centre of moment, has the regular geometric pattern and thus, this knowledge strengthens the results from this work.

Moreover, Barclay et al. [1978] and later Mather and Murdock [1994] has suggested that men have more shoulder swing and women have more hip swing if anatomical differences is to be used for recognition between men and women, suggesting the hip to be an important body part in gait recognition.

Results in this work also shows that whenever the combined data set is dependently extracted, which is extracted based on the most upper limb in the combination, the recognition rate is the highest among its data sets variations. Combined dataset dependently extracted means the knee and/or ankle angular displacements are extracted based on the hip or knee angle temporal information. They use similar temporal information, which makes it invariant to difference in time of start and end points leading to better recognition performance in comparison to independently extracted data. The independently extracted dataset has each angular displacement to have similar start and end points values, which are at the zero crossings. Hence, this work has been able to show that a difference in temporal information for different angular displacements does affect the recognition performance.

The result is not that surprising since work on model-based gait recognition such as the work of Yam [2002] and Yoo et al. [2003] have always used similar temporal information to reconstruct their gait model since the lower leg rotation parameters are formulated relative to the thigh rotation parameters at similar time instance. Wang et al. [2003] applies Dynamic Time Warping (DTW) to temporally align the signals of hip and lower leg rotation to a fixed reference phase for gait recognition. As is the work by Lakany [2000] on differentiating kinematics pattern of normal men to pathological men, similar temporal dynamics of the biomedical non-stationary signals of hip, knee, and ankle are used for generating the kinematics pattern. Also, research on modelling gait kinematics in the field of robotics employs similar method to formulate the gait kinematics model [Carlos et al. 2001].

Also, it is interesting to note that the recognition rate is highest when the number of nearest neighbours to the test data is 1. By analysing the feature spaces in Figure 4.4, Figure 4.6, and Figure 4.8, it is quite clear that each class has a large spread in its data distribution. Thus, neighbours of the same class are quite far away from each other.

4.3 Silhouette Moments Data

Silhouette moments data are calculated from silhouette images of size 720 x 576. These moment vectors, which represent sequences of image frames, are interpolated and resampled at sampling rate $r = 30$. Data sets consisting of different order moment vectors are built up of 10 subjects and 14 sequences for each subject. Table 4.2 displays the average correct classification rate for each simulation.

Only central moments as high as order 7 are considered in the simulations. This is due to the recognition performance, which seems to decrease after the experiment of dataset order up-to 5. This is clearly seen in Figure 4.9.

Table 4.2: Average Correct Classification of Silhouette Moments Data

Moments Order	$k = 1$	$k = 3$	$k = 5$
Order up-to 7	88.6 %	78.6 %	57.1 %
Order up-to 6	90.0 %	82.1 %	59.3 %
Order up-to 5	**90.7** %	85.0 %	62.9 %
Order up-to 4	90.0 %	**86.4** %	**65.7** %
Order up-to 3	90.0 %	82.9 %	62.9 %
Order up-to 2	89.3%	82.9%	62.1%
Order up-to 1	83.6%	70.0%	60.7%
Order 7	74.3%	61.4%	37.1%
Order 6	67.1%	54.3%	40.0%
Order 5	75.7%	60.7%	34.3%
Order 4	75.7%	66.4%	37.9%
Order 3	75.7 %	65.7%	35.0 %
Order 2	72.1 %	60.7 %	43.6 %
Order 1	53.6 %	39.3 %	24.3 %
Order 0	48.6%	46.4%	32.9%

Central moment of order 0 is just an area representation of the silhouette's region, which is highly dependent on the size of the silhouettes. Thus, the recognition rate for its silhouette moments data is the lowest among all simulations. It is about 49%.

Central moment of order 1 equals to zero. Hence, simulations of order **1** use the silhouette un-centralised moments data. However, only moment m_{01}, the vertical direction centroid has a periodic structure and this can be seen in Figure 3.8(c). Moment m_{01} also depends on height of the subjects being filmed. Moment m_{10}, the horizontal direction centroid, changes with the silhouette's displacement of the x-coordinates over the sequence (refer Figure 3.8(b)). This has been discussed in section 3.5.2. Thus, the recognition rate, which is about 54%, is still low in comparison to others.

From Table 4.2, the highest average classification rate is 90.7%, which comes from the simulations of all orders of silhouette moments data up-to order 5. Almost all combined silhouette moments data reached just above 80% recognition rate. In general, silhouette moments data of order 4 produce consistent high results in comparison to others. As the order of the silhouette moments data decreases, the recognition rate slowly decreases. This can be seen in Figure 4.9, which shows the performance change with change in moments order for different k numbers.

These values of recognition rate can be investigated by referring to its eigenvalues of the covariance matrix in PCA. In Figure 4.10, eigenvalues of silhouette data moments of order 2, order 3, order 4, and order 5 are displayed in a pareto plot. Figure 4.10(a) and (b) shows that the eigenvalues of the silhouette moments account for about two-thirds of the total variability in the data set, whilst Figure 4.10(c) and (d) has its eigenvalues account for about 90% and 80% of the total variability in the data set. Therefore, this high variance accountability has contributed to the higher recognition rate especially in the 4^{th} order silhouette moments data.

The choice for applying simple centralised moments to a silhouette dataset has been able to show that the silhouette moments have simple descriptive properties in producing distinct results for different temporal information of a silhouette dataset. Silhouette moments are simple to gather, invariant to translation due to different temporal information. It has an in built ability to discern, and filter, noise [Nixon and Aguado 2002]. The work by Shutler et al. [2000a] [2000b] has successfully applied velocity moments to silhouette data. As well as work by Lee and Grimson [2002a] [2002b]; this has applied centralised moments to gait dataset but using as many as 41 features. Further work on silhouettes, such as the work by Prismall et al. [2002] [2003] has managed to applied Legendre and Zernike moments to silhouette dataset for accurate reconstruction of moving silhouette. His work aims at predicting missing or intermediate frames within sequence.

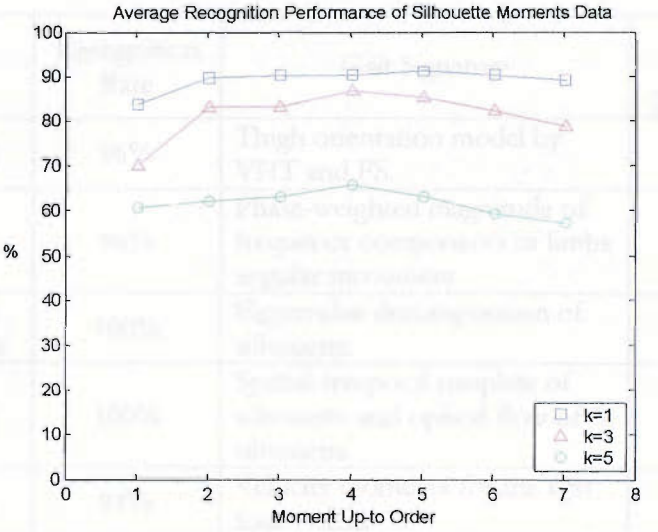

Figure 4.9: Average recognition performance of silhouette moments data.

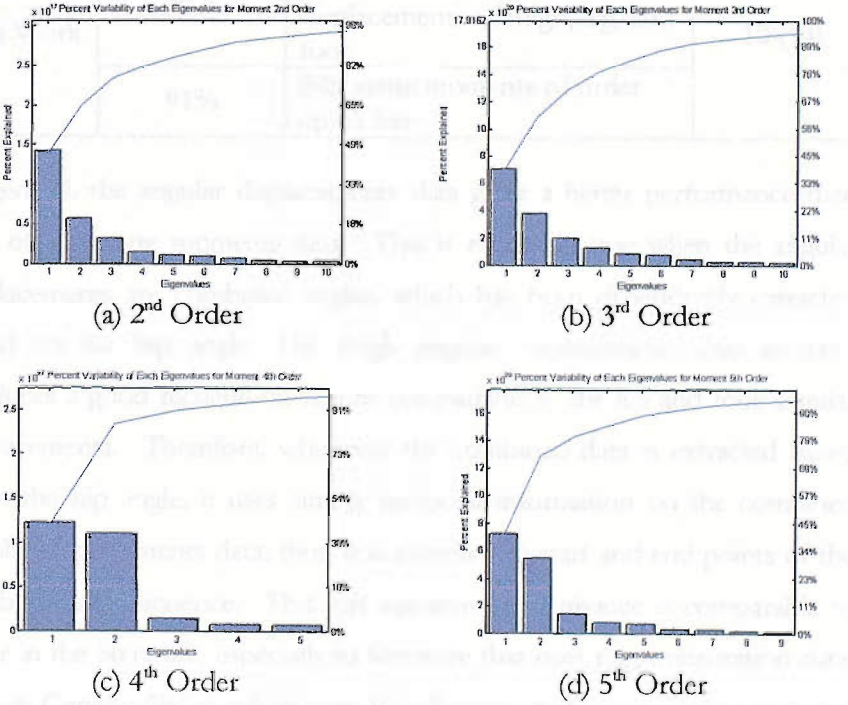

(a) 2nd Order (b) 3rd Order

(c) 4th Order (d) 5th Order

Figure 4.10: Percent variability of each eigenvalue of silhouette moments for different moments order.

4.4 Summary of Findings

Table 4.3: Comparison with Literature

	Recognition Rate	Gait Signature	No. of Subjects (Sequences)
Cunado	96%	Thigh orientation model by VHT and FS.	10 (4)
Yam	96%	Phase-weighted magnitude of frequency components of limbs angular movement.	5 (5)
Murase and Sakai	100%	Eigenvalue decomposition of silhouette.	7 (10)
Huang	100%	Spatial-temporal template of silhouette and optical flow of silhouette.	6 (4)
Shutler	94%	Velocity moments for the first four orders.	4 (4)
Lee and Grimson	100%	41 features of moments from orthogonal view.	24 (8)
This Work	98%	Dependently extracted combined angular displacements of thigh, leg, and foot.	10 (14)
	91%	Silhouette moments of order up-to five.	

In general, the angular displacements data gives a better performance than that of silhouette moments data. This is especially true when the angular displacements are combined angles, which has been dependently extracted based on the hip angle. The thigh angular displacements data in itself produces a good recognition rate in comparison to the leg and foot angular displacements. Therefore, whenever the combined data is extracted based upon the hip angle, it uses similar temporal information on the combined angular displacements data; thus, it is invariant to start and end points of the combined gait sequence. This gait signature performance is comparable to other in the literature, especially to literature that uses thigh orientation data, such as Cunado (96%), which uses 10 subjects with four sequences each and Yam (96%), which uses five subjects with five sequences each. The samples

used by both are small in comparison to this work; however, this work has been able to achieve better recognition rate performance.

Performance wise, silhouette moments data of the first five orders is a little far off in comparison to other literatures employing silhouettes, such as Murase and Sakai (100%), which uses seven subjects with 10 sequences each, and Huang (100%), which uses just six subjects with four sequences each, and literature employing moments, such as Lee and Grimson (100%), which uses 24 subjects with average eight sequences each. However, the gait signatures in the work of Murase and Sakai or Huang are applied to a smaller database compared to this work. While the work of Lee and Grimson uses moments extracted from seven regions of ellipses fitted to silhouettes, which differs slightly from this work in that this work considers the silhouette region as one whole region. Their work aims at recognising subjects by gait appearance, which requires the silhouette to be divided into regions in order to better describe change of appearance of subjects.

In comparing another analysis using moments, Shutler's work also produced 94% recognition rate using the first four order velocity moments, which are actually comparable to this work. Shutler's work actually uses the *Fisher* (*F*) statistic (from single factor Analysis Of Variance (ANOVA)) to identify which moments are more useful for classification purposes [Shutler 2000b]. In this work, even though the highest recognition rate achieved is from centralised order moments up-to order five but dataset of moments up-to order four has consistently produced high results. This is shown in Table 4.2 and Figure 4.9. Bare in mind that the *Fisher* (*F*) statistic in Shutler's work are applied to only four subjects with four sequences each, while this work uses a larger dataset. Thus, empirical result in this work has also shown that gait's silhouette dataset of order four and five can become a good descriptor for gait recognition.

Chapter 5

SUMMARY

"Physical reality consists of space-time events; no rational division into a 3-d space and a time continuum; laws of nature must correspond." [Einstein 1922]

5.1 Conclusions

Feature representation is an important element in feature extraction and thus, a feature should be as descriptive as possible to ensure success of classification. Within the realms of computer vision, gait is a new biometrics that recognises people by the way they walk. Gait kinematics features, which concerns its geometry, can be represented using its spatial and temporal characteristics; namely moments of silhouette and angular displacements of limb. Limb angular displacements data are hip angle, knee angle, and ankle angle and silhouette moments data are centralised moments of binary image data. In this work, the focus is on analysing gait kinematics features using data-driven approach.

A data-driven approach involves using extracted data and derivation of statistical information from the extracted data. In comparison to model-based approach, which is object-specific, data-driven approach aims at producing an informed decision on class labels of unseen data by processing it and testing it against systematically gathered and analysed past samples. It emphasises the understanding of functional relation of the sample data to the real world. Principal Component Analysis (PCA) and Canonical Analysis (CA) are techniques in feature extraction that uses statistical information of a dataset to produce good features for classification. To fit that purpose, PCA and CA analyse the variability in the data set to estimate its generalisation performance. PCA represents the dataset in a reduced dimensional space determined by the total covariance scatter and CA further discriminate the dataset using the within-class to between-class covariance scatters.

Combined features of angular displacements data and silhouette moments of a certain up-to orders have been used as signatures for analysing gait. The highest average recognition rate achieved is 98% for combined angular displacements data and 91% for silhouette moments data. Therefore, this work can suggest that angular displacements data, even though labour comprehensive, can be a better feature representation in comparison to the simple silhouette moments data.

5.2 Summary of Results

The research question of this work is on how descriptive is gait through analysing its kinematics features. This work has studied the spatial and temporal kinematics features of gait and has concluded that both features have the potential of being signatures for gait recognition. Below are the summarised results of this work and its contribution to the biometrics field:

- Temporal kinematics features of gait are the limb angular displacements data of the hip angle, knee angle, and ankle angle, which has been manually labeled and gathered to be feature vectors. Previous research in automatic gait recognition has used the angular displacements of hip and knee [Cunado et al. 1999] [Yam et al. 2002] [Yam 2002]. This work has introduced an extended feature by analysing the ankle angle, which is the foot flexion during a person's locomotion, in addition to the two commonly used features. Thus, the work has managed to show that the incorporation of ankle angle into the feature vectors can be used as signature in automatic gait recognition.

- Through the combination of angular features, analysis in this work has shown that the hip angle contains much of the variability during locomotion, which can contributes to the uniqueness of each person's gait. Thus, this evidence further strengthens research on automatic gait recognition if using angular displacements of the hip.

- Silhouette images are spatial features of gait. They are highly dimensional thus centralised moments have been used for its representation so as to be structurally similar with the feature vectors of angular displacements data. There are many research employing moments representation of silhouette but using different types of moments [Shutler et al. 2000a] [Prismall et al. 2002] [Prismall et al. 2003] and extracting moments from regions of silhouette [Lee and Grimson 2002a]. In this work, silhouette moments data has been analysed using the PCA and CA algorithm, which has been proposed by Huang [1999] but the method has been applied to a different content of the silhouette. Huang [1999] applied the algorithm to pixels and optical-flow of silhouette. Hence, this work has provided evidence that simple centralised moments of silhouette can become a gait feature for use in gait recognition.

- Before applying PCA and CA, the data needs to be pre-processed for making the analysis invariant for classification. Thus, a cycle extraction procedure, which involves interpolation and resampling, has been proposed in this work. This procedure has been shown to be a potential technique for introducing flexibility in gait recognition analyses, whereby it relieves the basis of defining complete gait cycle, which used to be defined at heel-strike in previous approach. It also reduces the data dimensionality hence eases the classification process.

5.3 Future Work

The work in this thesis concerns the analysis of kinematics features of gait using standard approaches; namely PCA and CA. There is much work for further research opportunity. Below are future works that can be suggested:

Feature Selection

Feature selection is a technique that chooses features but the ones more informative from the set of features. It identifies the most important and

relevant input variables that are responsible for major variations of the output. This technique uses search and filter strategies to gather, evaluate and select necessary gait features for analysis. In this work alone, two different types of gait features have been analysed. There are many other gait features that can be used for recognition but which features contribute to the best descriptive measure of gait recognition is still an open question.

Regression Analysis

This work has employed the SVR algorithm to interpolate the gait motion signal in the cycle extraction procedure. The SVR is an established method in machine learning, which has rigorous formulation and good generalisation capabilities. It employs implicit mappings of input data into the feature space via the kernel function. Thus, through this analysis, the affect of regularisation in the optimisation and interpolation using different kernel function can be explored. Also, this analysis can examine the effect of noise inclusion in the feature vectors for a more robust system.

Separability Measures Analysis

The separability measure that has been used in this work is the ratio of within-class and between-class scatter of gait dataset. Therefore, through the separability measures analysis, several separability measures can be used and formulated for feature discrimination. The analysis can evaluate and decide on the best separability measures for measuring performance of gait.

Occlusion Analysis

The manual labelling of the angular displacements data has been applied onto the leg nearest to the camera view (i.e. outer leg). Thus, analysis on occlusion will investigate the occluded (inner) leg of gait data. It can explore gait symmetry by studying the effect of using either outer leg, or inner leg, or both legs as gait descriptors.

BIBLIOGRAPHY

Alon, N., S. Ben-David, N. Cesa-Bianchi, and D. Haussler (1997). Scale-sensitive dimensions, uniform convergence, and learnability. *ACM 44* (4), 615–631.

Abdelkader, C., R. Cutler, and L. Davis (2002a, June). View-invariant estimation of height and stride for gait recognition. *Proceedings International ECCV Workshop*, 155-167.

Abdelkader, C., R. Cutler and L. Davis (2002b). Motion-based recognition of people in eigengait space. *5th International Conference on Automatic Face and Gesture Recognition.*

Ayyappa, E. (1997). Normal human locomotion, part 1: basic concepts and terminology. *Journal of Prothestics and Orthotics 9* (1), 10-17.

Barclay, C.D., J.E. Cutting, and L.T. Kowzlowski (1978). Temporal and spatial factors in gait perception that influence gender recognition. *Perception and Psychophysics*, 23, 145-152.

Belhumeur, P.N., J.P. Hespanha, and D.J. Kriegman (1997, July). Eigenfaces vs. fisherfaces: recognition using class specific linear projection. *IEEE Transactions on Pattern Analysis and Machine Intelligence 19* (7), 711-720.

Bellman, R.E. (1961). *Adaptive Control Processes.* Princeton University Press.

Beveridge, J.R., K. She, B.A. Draper, and G.H. Givens (2001). Nonparametric statistical comparison of principal component and linear discriminant subspaces for face recognition. *Computer Vision and Pattern Recognition.*

Bhanu, B. and J.Han (2003). Human recognition on combining kinematic and stationary features. *Proceedings 4th AVBPA*, 140.

Bradley, P.S., O. L. Mangasarian, and W. N. Street (1995). Feature selection via mathematical programming. *INFORMS Journal on Computing 10* (2), 209–217.

Carlos, M.B., J.A. Rodrigues, and T. Machado (2001, May 21-26). A Fourier perspective in multi-legged systems. *IEEE International Conference on Robotics and Automation.*

Chambers, H.G. and D.H. Sutherland (2002, May/June). A practical guide to gait analysis. *Journal of the American Academy of Orthopaedic Surgeons 10* (3), 222-231.

Chen, L. and H. Man (2003). Combination of Fisher scores and appearance based features for face recognition. *Proceedings of the 2003 ACM SIGMM Workshop on Biometrics Methods and Applications.* 74-81.

Cherkassky, V. and F. Mulier (1998). *Learning from Data: Concepts, Theory, and Methods.* John Wiley I & Sons Publishing.

Cunado, D., J. M. Nash, M. S. Nixon, and J. N. Carter (1999, March). Gait extraction and description by evidence-gathering. *Proceedings 2nd AVBPA*, 43–48.

Cutting, J.E. and D.R. Profitt (1981). Gait perception as an example of how we perceive events. R.D. Walk and H.L. Pick (Eds.), *Intersensory Perception and Sensory Integration.* London: Plenum Press.

Cutting, J.E., D.R. Profitt, and L.T. Kozlowski (1978). A biomechanical invariant for gait perception. *Journal of Experimental Psychology: Human Perception and Performance*, 4, 357-372.

Davis, J. W. (2001, June). Visual categorisation of children and adult walking styles. *Proceedings 3rd AVBPA*, 295–300.

Ehrenberg, A.S.C. (1989). *A Primer in Data Reduction: An Introductory Statistics Textbook.* John-Wiley I & Sons Publishing.

Einstein, A. (1922, 1st edition). *The Meaning of Relativity*, Princeton, New Jersey, Princeton University Press.

Eng, J.J. and D.A. Winter (1995). Kinetic analysis of the lower limbs during walking: What can be gained from a three-dimensional model? *Journal of Biomechanics 28*, 753–758.

Foster, J.P., M.S. Nixon, and A. Prugel-Bennett (2001, June). New area based metrics for gait recognition. *Proceedings 3rd AVBPA*, 312–317.

Frigo, C., D. Eng, and L. Tesio (1986). Speed-dependent variations of lower-limb joint angles during walking. *American Journal of Physical Medicine 65* (2), 51–62.

Gleason, A. (2001). *Who is Fourier? A Mathematical Adventure (5th edition).* 68, Leonard Street, Suite 9, Belmont, MA: Language Research Foundation. English Version.

Grieve, D.W. and R.J. Gear (1966). The relationship between length of stride, step frequency, time of swing and speed of walking children and adults. *Ergonomics 14* (5), 379-399.

Gonzales, R.C. and R.E. Woods (1992). *Digital Image Processing.* Addison-Wesley Publishing Company.

Gunn, S.R. (1998, March). MATLAB Support Vector Machine Toolbox. (Internet).

Gunn, S.R. and J.S. Kandola (2001). Structural modelling with sparse kernels. *Machine Learning.*

Hills, A.P. and A.W. Parker (1993). Gait characteristics of obese children. *Architecture Phys Medical Rehabilitation 72*, 403-407.

Hu, M.K. (1962, February). Visual pattern recognition by moment invariant. *IRE Transactions on Information Theory IT-8*, 179-187.

Huang, P.S, C.J. Harris, and M.S. Nixon (1999). Human gait recognition in canonical space using temporal templates. *IEE Proceedings: VISP 146* (2), 93–100.

Huang, P.S. (1999). *Automatic Gait Recognition via Statistical Approaches.* Ph.D. thesis, School of Electronics and Computer Science, Faculty of Engineering, Science and Mathematics, University of Southampton.

Inman, V.T., H.J. Ralston, and F. Todd (1981). *Human Walking.*Williams and Wilkins.

Jain, A.K. (1989). *Fundamentals of Digital Signal Procesing.* Prentice Hall.

Jain, A.K. and R.C. Dubes (1988). *Algorithms for Clustering Data.* Prentice Hall.

Jain, A.K., R. Bolle, and S. Pakanti (1999). *Biometrics - Personal Identification in Networked Society.* Kluwer Academics Publishers.

Johansson, G. (1973). Visual perception of biological motion and a model for its analysis. *Perception and Psychophysics 12.*

Johnson, A.Y. and A.F. Bobick (2001, June). A multi-view method for gait recognition using static body parameters. *Proceedings 3rd AVBPA*, 301–311.

Kandola, J.S. (2001). *Interpretable Modelling with Sparse Kernels.* Ph.D. thesis, School of Electronics and Computer Science, Faculty of Engineering, Science and Mathematics, University of Southampton.

Kozlowski, L.T. and J.E.Cutting (1977). Recognising the sex of a walker from dynamic point-light display. *Perception and Psychophysics 21* (6), 575–580.

Lakany, H.M. (2000). A generic kinematic pattern for human walking. *Neurocomputing 35*, 27-54.

Lee, L and W.E.L. Grimson (2002a, May). Gait analysis for recognition and classification. *Proceedings of the 5th IEEE International Conference on Automatic Face and Gesture Recognition.*

Lee, L. and W.E.L. Grimson (2002b, June). Gait appearance for recognition. *Proceedings Biometrics Authentication International ECCV Workshop*, 143-154.

Little, J. and J. Boyd (1998). Recognising people by their gait: The shape of motion. *Videre: Journal of Computer Vision Research 1* (2), Article 1.

Martinez, A.M. and A.C. Kak (2001, February). PCA versus LDA. *IEEE Transaction on Pattern Analysis and Machine Intelligence 23* (2), 228-233.

Mather, G. and L. Murdoch (1994). Gender discrimination in biological motion displays based on dynamic cues. *Proceedings R. Soc. London B*(258), 273–279.

Mowbray, S.D. and M.S. Nixon (2003). Automatic gait recognition via Fourier descriptors of deformable objects. *Proceedings AVBPA*, 566-573.

Murase, H. and R. Sakai (1996). Moving object recognition in eigenspace representation: Gait analysis and lip reading. *Pattern Recognition Letters 17*, 156–162.

Murray, M.P. (1967). Gait as a total pattern of movement. *American Journal of Physical Medicine 46* (1), 290-332.

Murray, M.P., A.B. Drought, and R.C. Kory (1964). Walking patterns of normal men. *Journal of Bone and Joint Surgery 46-A* (2), 335-360.

Nixon, M.S., A.S. Aguado (2002). *Feature Extraction in Computer Vision and Image Processing.* Newnes.

Nixon, M.S., J.N. Carter, D. Cunado, P.S. Huang, and S.V. Stevenage (1999). Automatic Gait Recognition. *BIOMETRICS – Personal Identification in Networked Society*, A.K. Jain, et al. Eds., 231-249, Kluwer Academic.

Niyogi, S.A. and E.H. Adelson (1994). Analysing and recognising walking figures in xyt. *Proceedings Conference CVPR*, 469–474.

Perry, J. (1992). *Gait Analysis: Normal and Pathological Function*, SLACK, NJ.

Phillips, P., H. Moon, P. Rauss, and S. Risvi. (1997). The FERET evaluation methodology for face-recognition algorithms. *Proceedings CVPR*, 137-143.

Prismall, S.P., M.S. Nixon, and J.N. Carter (2002). On moving object reconstruction by moments. *Proceedings BMVC*, 1-10.

Prismall, S.P., M.S. Nixon, and J.N. Carter (2003). Accurate object reconstruction by statistical moments. *Proceedings of VIE*, 1-5.

Saunders, J.B., V.T. Inman, and H.D. Eberhart (1953). The major determinants in normal and pathological gait. *Journal of Bone and Joint Surgery 35-A*, 543-558.

Schölkopf, B. (1998). Statistical learning and kernel methods. *Proceedings of the 1998 NIPS Workshop on Kernel Methods.*

Schölkopf, B. (2000). *Statistical Learning and Kernel Methods.* Technical Report MSRTR- 2000-23, Microsoft Research.

Shaknarovich, G., L. Lee, and T. Darrell (2001). Intergrated face and gait recognition from multiple views. *Proceedings CVPR.*

Shutler, J.D., M.S. Nixon, and C.J. Harris (2000a). Statistical gait description via temporal moments. *Proceedings SSIAI*, 291-295.

Shutler, J.D., M.S. Nixon, and C.J. Harris (2000b). Statistical gait recognition via velocity moments. *Proceedings IEE Colloquium: Visual Biometrics* (00/018), 11/1-11/5.

Shutler, J.D., M.G. Grant, M.S. Nixon, and J.N. Carter (2002, December). On a large sequence-based human gait database. *Proceedings RASC*, Nottingham, UK.

Smola, A.J. (1996). Regression estimation with support vector learning machines. Technical report, Technische Universit¨at M¨unchen.

Stevenage, S.S., M.S. Nixon, and K. Vince (1999). Visual analysis of gait as a cue to identity. *Applied Cognitive Psychology 13*, 513–526.

Swartz, J. (1999). The growing "magic" of automatic identification. *IEEE Robotics and Automation Magazine 1070* (9932), 20–23.

Swets, D.L. and J.J. Weng (1996, August). Using discriminant eigenfeatures for image retrieval. *IEEE Transaction on Pattern Analysis and Machine Intelligence 18* (8), 831–836.

Tham, M.T. (1997, April. Last modified, February 2001). An introduction to SPC. http://lorien.ncl.ac.uk/ming/spc/copyspc.htm.

Thomson, D.M. (1998, May 18 last updated). The determinants of normal and pathological gait http://moon.ouhsc.edu/drhompso/gait/knmatics/saunders.htm.

Turk, M. and A. Pentland (1991). Eigenfaces for recognition. *Journal Cognitive Neuroscience 31* (1), 71–86.

Vapnik, V. (1995). *The Nature of Statistical Learning Theory.* Springer-Verlag Publishing New York.

Wang, L., H. Ning, T. Tan, and W. Hu (2003). Fusion of static and dynamic body biometrics for gait recognition. *Proceedings of the Ninth IEEE International Conference on Computer Vision.*

Webb, A. (1999). *Statistical Pattern Recognition.* Arnold.

Wolberg, G. and I. Alfy (2002). An energy-minimisation framework for monotonic cubic spline interpolation. *Journal of Computational and Applied Mathematics* 143, 145– 188.

Yam, C.Y. (2002, November). *Model-Based Approaches for Recognising People by the Way They Walk or Run.* Ph.D. thesis, School of Electronics and Computer Science, Faculty of Engineering, Science and Mathematics, University of Southampton.

Yam, C.Y., M.S. Nixon, and J.N. Carter (2001, June). Extended model-based automatic gait recognition of walking and running. *Proceedings 3rd AVBPA 2001* , 278–283.

Yoo, J., M.S. Nixon, and C.J. Harris (2002). Model-driven statistical analysisi of human gait motion. *Proceddings of ICIP 1*, 285-288.

Yoo, J. and M.S. Nixon (2003). On laboratory gait analysis via computer vision. *Proceedings AISB Symposium on Biologically-Inspired Machine Vision, Theory, and Application*, 109-113.

Young, T.Y. and K. Fu. (1986). *Handbook of Pattern Recognition and Image Processing.* Academic Press.

Zhao, W., P.J. Phillips, and R. Chellappa (2000). Subspace linear discriminant analysis for face recognition. *IEEE Transactions on Image Processing.*

Zhao, W., R. Chellappa, and A. Krishnaswamy (1998). Discriminant analysis of principal components for face recognition. *Proceedings of the 3rd International Conference on Face and Gesture Recognition.* 336.